CHALMERS
UNIVERSITY OF TECHNOLOGY

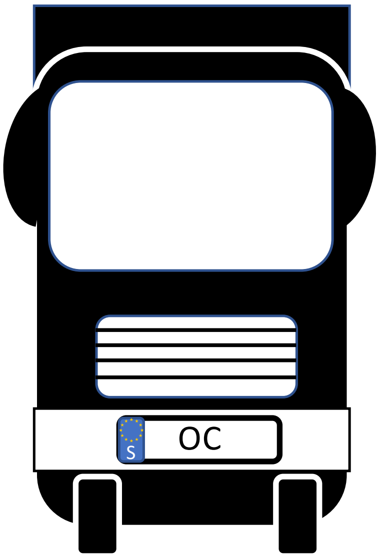

Assessing the feasibility of replacing a specific diesel truck with a Battery Electric Vehicle using the Operating Cycle format

Master's thesis in Systems, control and mechatronics, MSc

CARL EMVIN

Department of Mechanics and Maritime Sciences
CHALMERS UNIVERSITY OF TECHNOLOGY
Gothenburg, Sweden 2023

MASTER'S THESIS IN SYSTEMS, CONTROL AND MECHATRONICS

Assessing the feasibility of replacing a specific diesel truck with a Battery Electric Vehicle using the Operating Cycle format

CARL EMVIN

Department of Mechanics and Maritime Sciences
Division of Vehicle Engineering and Autonomous Systems
Vehicle Dynamics group
CHALMERS UNIVERSITY OF TECHNOLOGY
Gothenburg, Sweden 2023

Assessing the feasibility of replacing a specific diesel truck with a Battery Electric Vehicle using the Operating Cycle format

CARL EMVIN

Master's Thesis
Department of Mechanics and Maritime Sciences
Division of Vehicle Engineering and Autonomous Systems
Vehicle Dynamics group
Chalmers University of Technology
SE-412 96 Göteborg
Sweden
Telephone: + 46 (0)31-772 1000

Examiner: Bengt Jacobson
Supervisor: Fredrik Bruzelius, Rickard Andersson, Luigi Romano

Department of Mechanics and Maritime Sciences
Gothenburg, Sweden 2023-02-27

Assessing the feasibility of replacing a specific diesel truck with a Battery Electric Vehicle using the Operating Cycle format

Master's thesis in Systems, control and mechatronics, MSc
CARL EMVIN
Department of Mechanics and Maritime Sciences
Division of Vehicle Engineering and Autonomous Systems
Vehicle Dynamics group
Chalmers University of Technology

Abstract

While facing continuously stricter legislation due to the threat of global warming, vehicle manufacturers strive to find alternative means of transportation such as the *Battery Electric Vehicle* (BEV). While doing so, uncertainties regarding performance are halting the shift to more sustainable alternatives.

This thesis will therefore build a framework for retailers to predict and estimate to which degree a BEV can replace a fossil-driven vehicle in specific missions. The framework will try to describe the details of transport missions while remaining relatively computationally light. This framework developed within the COVER project is called *Operating Cycle* (OC). It is a description of a road transport mission with an adequate level of detail that captures the physical and practical phenomenon of a transport mission. It can be divided into two sub-descriptions, the *deterministic Operating Cycle* (dOC) and *stochastic Operating Cycle* (sOC), which are the representations adopted in this thesis. Using vehicle log data from a specific *Internal Combustion Engine Vehicle* (ICEV), the OC format is extended to include models for **Payload, Mission stop and EV-Recharging**. Using the models of the OC format, a feasibility analysis of replacing a specific vehicle with a BEV is conducted. The resulting analysis shows that the current BEV fleet is not able to complete all the missions that the ICEV completed without alteration of specific transport missions.

Keywords: Operating Cycle, Stochastic modelling, Transport mission, Battery Electric Vehicle, Depth of Discharge, State of Charge, deterministic Operating Cycle

Contents

Preface

This thesis has studied field log data acquired from September 2020 to August 2021, spanning exactly one year. The models developed using the data will be a part of the OC format developed within the COVER project with the result of describing a transport mission. The project is carried out at the Department of Mechanics and Maritime Sciences, Vehicle dynamics, Chalmers University of Technology, Sweden. The project is a close collaboration between industry and research with industry partners such as Volvo Group.

A special thanks to Luigi Romano for guidance in model development and knowledge sharing of the OC format. Also, thanks to Fredrik Bruzelius and Bengt Jacobson for helping me understand the field of vehicle dynamics. I have accumulated a lot of interesting knowledge through discussions with you that have made the thesis what it is. From Volvo's side, a special thanks to Rickard Andersson. Your guidance of the Volvo architecture including, systems, knowledge and ideas have been priceless.

Gothenburg, 2023-02-27

CARL EMVIN

Notations

Symbol	Explaination
OC_s	stochastic Operating Cycle parameters
R_s	Stochastic road parameters
W_s	Stochastic weather parameters
T_s	Stochastic traffic parameters
M_s	Stochastic mission parameters
X_k	Random variable
$\mathcal{E}(\cdot)$	Exponential distribution
λ_s	Sign intensity
T_k	Standstill time stochastic variable
$u(\cdot)$	Uniform distribution
t_{min}	Lower boundery for standstill time
t_{max}	Upper boundery for standstill time
V_k	Recommended speed stochastic variable
v_{min}	Lower boundary for recommended speed
v_{max}	Upper boundary for recommended speed
P	Proability
S_V	Collection of possible speed signs
p_{Vij}	Probability of transition from state i to state j
f_{Vij}	Number of transitions from state I to state j.
$AR(\cdot)$	Autoregressive
$MA(\cdot)$	Moveing average
$I(\cdot)$	Integration
Y_k	Road grade random variable
ϕ_Y	AR(1) model parameter
L_h	Hill length
σ_{eY}^2	Error variance
C_k	Curvature random variable
r_{turn}	Minimum curvature radius
μ	Mean
μ_T	Mean temperature
μ_Ψ	Mean relative humidity
T_y	Annual trend amplitude, temperature
Ψ_y	Annual trend amplitude, relative humidity
ω_y	Annual frequency
ω_d	Daily frequency
Ψ_d	Daily trend amplitude, relative humidity
T_d	Daily trend amplitude, temperature
φ	Phase angle
$\tilde{T}_k$	Stochastic variable for temperature
$\tilde{\Psi}_k$	Stochasitc variable for relative humidity
$\mathrm{ARIMA(p, d, q)}$	Autoregressive integrated moving avarage
$\phi_P(L)$	Autoregressive lag polynomial
c_P	drift
$H_{p,k}$	Descrete random variable for precipitation
$Ga(\alpha, \beta)$	Gamma distribution
$\mathbf{Y}_{w,k}$	Wind speed and direction vector.

c_w	Constant offset
$\boldsymbol{\Phi}_w(L)$	Matrix operator
$\rho_t(x,t)$	Traffic density
$v_t(x,t)$	Traffic speed
$q_t(x,t)$	Traffic flow
v_e	Vehicle speed
v_f	Free flow speed
α	Scale parameter, (first shape parameter for stable distributions)
β	Shape parameter
γ	Scale parameter
δ	Location parameter
μ	Location parameter
σ	Scale parameter
ν	Shape parameter
T	Threshold
T_k	Connector type
P_{init}	Initial state probabilities
$\Gamma(\cdot,\cdot)$	Gamma distribution
P_k	Max charge power
$C_{c,k}$	Capacity (number of connectors)
P_0	Probability of zero vehicles in the system.
L_s	Average number of vehicles in the system
W_s	Average time spend in the system
L_q	Average number of vehicles in the queue
W_q	Average time spend in the queue
$W_{s,vehicle}$	Estimated time spend in the system for the simulated vehicle.
E_{req}	Requested energy
ω	Weights
B_i	Sequence of consecutive identical samples.

List of Acronyms

OC	-	Operating Cycle
dOC	-	Deterministic Operating Cycle
sOC	-	Stochastic Operating Cycle
GCW	-	Gross Combination Weight
AR	-	Autoregressive
MA	-	Moving average
ARIMA	-	Autoregressive integrated moving average
BEV	-	Battery Electric Vehicle
ICEV	-	Internal Combustion Engine Vehicle
HD	-	Heavy Duty
IEA	-	International Energy Agency
EV	-	Electric vehicle
SoC	-	State of Charge
DoD	-	Depth of Discharge
VECTO	-	Vehicle Energy Consumption calculation TOol

1 Introduction

This thesis is examining the feasibility of replacing a specific ICEV with a BEV. The introduction gives a thorough exposition of the problem formulation, background and methods used throughout this thesis.

1.1 Background

Many countries and regions have taken on the climate challenge by setting goals to reduce carbon dioxide from transport. Quantifying and reducing carbon dioxide emissions is not only a requirement by legislation but also a customer need for many. Trivially, companies strive to match the market needs but a survey given to 1.500 corporate executives found that 70% of those surveyed indicated that their company had not made a clear case towards sustainability by 2009 [1]. The study also indicated that sustainability initiatives usually are compliance-driven rather than strategic, thus the lack of well-defined sustainability projects. Unlike most initiatives, this thesis tries to find sustainable solutions that have a possibility of being profitable for companies. Not only to meet customer needs and legislation but also by distributing the optimal vehicle concerning vehicle use.

As mentioned, the transport sector faces multiple emission-related legislations and will likely continue to do so in the future. It is therefore necessary to present the laws and targets that the vehicle industry must obey in the nearest future. Sweden has recently (2018) decided on climate goals targeted towards transportation. Swedish authorities demand a CO_2 reduction of 70% within the transportation sector over two decades (2010 to 2030) [3]. EU demands an emissions reduction from newly produced heavy vehicles of 30% from the year 2030 [5] onwards. The reduction is compared against reference CO_2 emissions based on monitoring data from the period 1st of July 2019 to 30th of June 2021. To remain competitive within the vehicle industry one will therefore have to find a solution that complies with the climate goals that exist and will exist going forward.

Except for legislation, there exist ethical problems with burning fossil fuels. The continents that have the highest $C0_2$ emissions per capita are generally not those that suffer from the consequences [8]. The article states that a two-degree increase in average temperature would risk putting half of Africa's population at risk of undernourishment. Also, multiple studies manifest that the world must make a change in trajectory concerning CO_2 emissions to avoid causing irreversible damage to certain ecosystems. To quantify the impact of greenhouse gases, Nasa argues that the average temperature has risen about 1 degree C since 1880 [6]. Given the increase in $C0_2$ emissions, see Figure 1-1, one might argue that our current trajectory is pointing towards a warmer earth (except for the COVID pandemic year 2020).

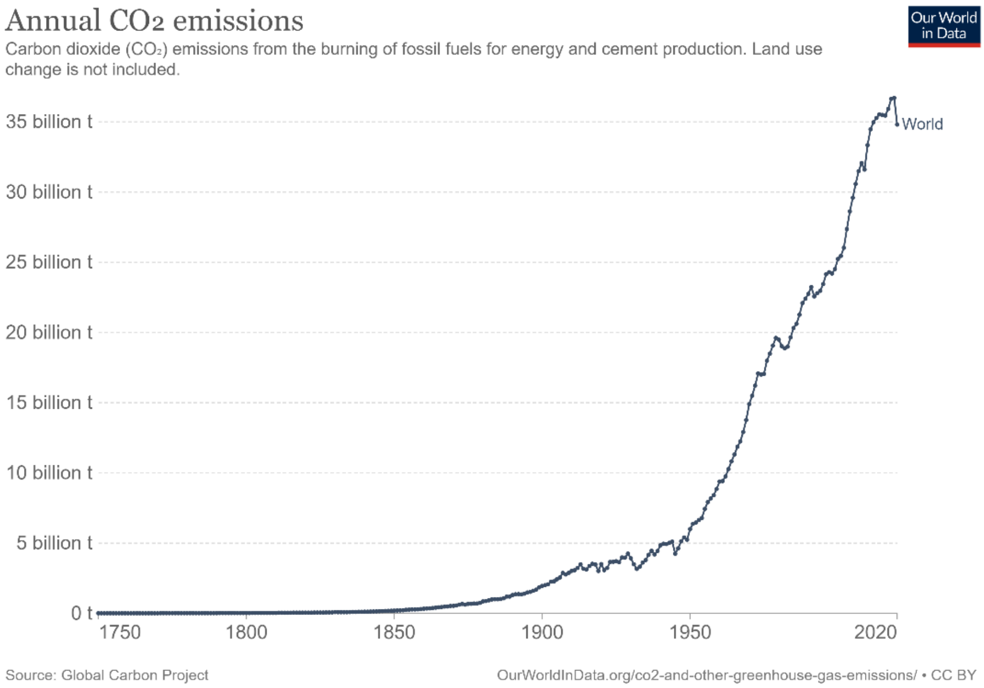

Figure 1-1. Annual CO2 emissions worldwide [6].

To quantify, predict and analyse $C0_2$ emissions from the transportation sector there have been numerous initiatives, but an important one is the *Vehicle Energy Consumption calculation TOol* (VECTO) [2] developed by the European commission. Although very precise concerning $C0_2$ emissions and energy consumption, it does lack variation and has a risk of consolidating old technical solutions. The software includes 5 reference missions that are used in the quantification of vehicle emissions. The actual energy consumption of vehicles depends on vehicle use and does therefore not always follow the declared values. The automotive industry has for a long time searched for suitable methods and mathematics to describe transport assignments and actual vehicle use. A description of a transport mission developed through the COVER project is the OC. The OC format can be divided into two parts, deterministic OC and stochastic OC and can be further read about in Chapter 2.

Except for the sustainability aspect, there are strategic reasons to reduce the spill of certain minerals and materials. Material shortage is currently not a big problem for the vehicle industry, except for certain components, but with the rise of BEV and battery-driven technology, the IEA predicts the lithium market to have supply shortages as soon as 2025 [4] which inevitably will drive up the prices and disrupt the supply chain. Another study written by USGS [14] expects the Lithium world reserve to be 22 million tonnes, which corresponds to two hundred twenty times the production volume of 2021. But the problem is not that there is too little lithium on planet earth, it is the rate of production that IEA argues cannot with current technology keep up with future needs. It is therefore in everyone's interest to minimize lithium redundancy in product deployment and in the future find a sustainable means of recycling old batteries.

Apart from developing good sustainable products, companies must convince haulages and customers that their missions are better operated by the BEV rather than an ICEV to meet the climate targets set by the EU. Haulages have relied on ICEVs since time immemorial and do need incentives to make a shift. By facilitating an answer to the question "*Can a BEV replace my ICEV without altering my transport missions?",* consumers should feel more secure in the transition to BEVs. The answer to that question is to be investigated in the present thesis, *Virtual study of an electric heavy-duty vehicle in real operation*.

1.2 Problem motivating the project

As mentioned in Section 1.1, there are numerous reasons for the transport sector to develop a market-leading non-fossil fleet. In the transition from internal combustion engine vehicles (ICEV) to battery electric vehicles (BEV), consumers are questioning the reliability of the new BEVs. To assess the problem, a detailed description of vehicle use is required, a description that is robust enough to function when the access to road data is limited and detailed enough to give a valuable result.

1.3 Envisioned solution

The thesis provides a skeleton solution for how heavy vehicles can be tailored to their usage. The skeleton solution makes use of previous work written within the COVER project as well as contributes to the format with new models. Specifically, source code and theory developed by Erik Nordström [9], Luigi Romano [10] and Pär Pettersson [11] to name some of the contributors. This thesis contributes by incorporating 3rd party data in the OC format such as weather and road data. All of this is packaged into an automized process that by as little interaction and modifications as possible can be run in another setting, for example, using data from another haulage.

1.4 Objective

The main objective of this study is to investigate to what extent a specific customer can utilize a BEV to accomplish their transport missions with success compared to today's diesel-based fleet using a further developed OC format.

1.5 Deliverables

- A description of the
    - current sOC implementation.
    - contributions from the present thesis to the OC format, specifically within the mission property.
- An analysis
    - using large samples of vehicle log data, specifically *Gross Combination Weight* (GCW) and mission stops.
    - of simulation results using dOCs. For example, energy consumption and mission failure/success rate.
- A framework consisting of models, methods and tools that are reusable in another setting. For example, using log files from another haulage with different vehicles.

- Sizing of the battery pack with respect to the accessibility of charging stations for a specific customer.
- Integration of road and weather data from 3rd party data suppliers into the dOC format. For example, altitude, air density and road signs.

1.6 Limitations

- The data processed was recorded by one single truck between the fall of 2020 to the fall of 2021. Third-party road data deliveries do not consider the date of recording, so there is a possibility that the road data retrieved is misrepresentative for certain parts of a mission.
- The weather data are recorded at Landvetter flygplats as opposed to the road-specific values one would like to have. Also, the data is recorded every hour with data losses being a commonality.
- Working with big data requires the simulations to be robust and fast. Some functionalities are not possible to have. For example, a complex tyre model.
- The result from this thesis is a product of the data collected by one vehicle and simulated using one vehicle model. Other vehicles and vehicle models might produce different results.

1.7 Method

This Section will describe the different methods that will be used throughout this thesis. Here it is important to distinguish between mission framework and transport mission. Mission framework refers to the start and end of a transport mission, whereas the transport mission represents everything affecting the vehicle under operation.

1.7.1 Mission framework definition

Previous theses written within the same project, the COVER project, have defined the framework of a mission as the start to the end of a log file, where the data logging starts and stops when the engine does so. In contrast, this project will allow a mission to be considered as a whole day of work. This mission framework exposes BEV-specific problems that an ICEV would not encounter. Such problems are lack of charging infrastructure or lack of range given a specific battery-pack size. These problems arise for BEVs as a consequence of recharging being a slow operation in comparison to refuelling for ICEVs. Also, assuming that the vehicle is not in operation during the night, the BEV is always considered fully recharged at every mission start. The assumption holds for haulages with a recharging point which is reasonable to demand given they own a BEV. This mission definition enables the use of a previously unused property within the OC format, the mission property. This property describes changes in payload, recharging, mission stops, etc. For further reading of the mission property, the author refers to Section 3.2 and Section 3.3

1.7.2 Transport mission descriptions

A transport mission can be represented in numerous ways, to mention a few of them: There is the bird’s eye view, the dOC and the sOC. The bird's eye view description is conceived to be the most general, allowing straightforward classification of transport missions. In contrast, the sOC is a mid-level representation describing a transport mission through its stochastic parameters and models. The models give insight into variations in altitude profiles, curviness, traffic etc. that the other transport mission descriptions cannot provide. Lastly, the dOC representation is a low-level description of a transport mission which captures the details of a specific mission. The upside of the dOC format is that it can act as input to full vehicle simulations making it possible to retrieve estimates of energy consumption, velocity profiles, etc. The dOC and sOC description will throughout this project remain the core concepts of this thesis.

1.7.3 Model development

In the development of models for the sOC and dOC, three core methods are used. First, in the development of the models, log data are examined to give information regarding the characteristics of the signal. Such signals are the GCW signal and the Boolean trailer-connected signal. Second, grey box models are built using the information gained through the data analysis together with the existing knowledge base within each system. Third, model parameters are fitted using a set of data covering one year.

1.7.4 Simulation model library

The simulation model library used in this thesis is *VEHicle PROPulsion* (VehProp), developed at Chalmers. VehProp is a simulation model library for vehicle operations where one can execute full vehicle simulations to retrieve estimates of energy consumption and velocity profiles to name a few. In this thesis, VehProp assists in the feasibility analysis of replacing a specific ICEV with a BEV. One version of VehProp accepts the operating cycle format as input to the environment, making VehProp suitable for this study.

1.7.5 Stochastic models

In model development and the analysis of simulation results, well-established stochastic processes are often assumed. Such are Gaussian, Poisson, and gamma processes. Simplicity is not a direct requirement for this thesis, though, one must be able to draw samples from the distributions, preferably using built-in MATLAB functions. Also, it is of interest to make the models generic to ease future work within the field.

2 Operating Cycles

This chapter presents the OC format without any of the contributions from the present thesis. Those are instead presented in chapter 3.

2.1 The deterministic operating cycle

The dOC describes a specific transport mission. It can either be a product of vehicle log data/external road data or it can be generated from an sOC. The dOC format is just as it sounds, deterministic, and has the possibility of being used as input to simulations. After simulation with dOC input, one can investigate how different vehicle configurations and driving behaviours affect energy consumption. The dOC format was originally developed by Pär Pettersson and is presently being further developed by Luigi Romano. A table of all the parameters included in the current dOC format is presented in Table 2-1

Table 2-1. dOC parameters. The first column of each parameter is distance. The quality of the data acquired varies. Also, Traffic density can be generated from the sOC model.

	Description	Unit	Data acquired
Road:			
Topography:	Altitude	(m)	Y
Legal speed:	Speed limit	(m/s)	Y
Curvature:	Radius of circle segment	(1/100 meter)	Y
Stop sign:	Standstill time	(s)	Y
Latitude:	WGS84 latitude	(degree)	Y
Longitude:	WGS88 longitude	(degree)	Y
Ground type:	Surface type, cone index	(-, kPa)	N
Roughness:	waviness, roughness coef. (ISO 8608)	(-, m^3)	Y
Speed bump:	Length, eight, angle	(m, m, degree)	Y
Traffic light:	Standstill time	(s)	Y
Give way sign:	Recommended speed	(m/s)	N
Traffic:			
Traffic density:	Density	(cars/m)	N
Mission:			
Payload:	GCW – kerb weight = Payload	(kg)	Y
EV-Recharging:	Power	(watt)	Y
Power take off:	Time	(s)	Y
Travel direction:	(1=forward, 0=reverse)	(boolean)	Y
Mission Stop:	Standstill time (engine turned off)	(s)	Y
Mission matrix:	Composition of Mission parameters	(Boolean, kg, watt, watt, Boolean, s)	Y
Weather:			
Ambient temperature:	Temperature	(degrees Celcius)	Y
Wind velocity:	Wind velocity (speed and angle)	(degree, m/s)	Y
Relative humidity:	Moisture content in air relative to possible moisture content in air.	(%)	Y
Atmospheric pressure:	Air pressure	(hPa)	Y

2.2 The stochastic operating cycle

The stochastic operating cycle (sOC) is a mid-level description of a transport task. It ideally spans the whole set of models that describe a transport mission. The set of models and parameters required can be split into four different categories: *road, weather, traffic, and mission.* Each category includes several secondary models, such as the topography and curvature model and some of these models do inherit statistical parameters from their primary model. The structure of the sOC format is best described in Figure 2-1.

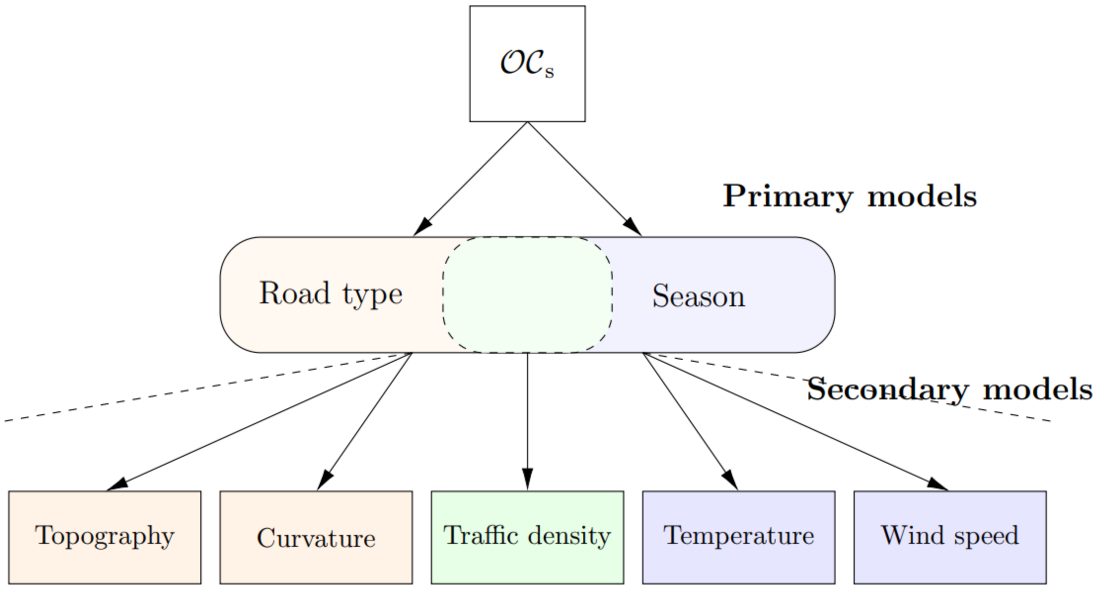

Figure 2-1. Hierarchical structure of an sOC. Road type and season are both primary models and influence the value of the statistical parameters for the secondary models. Whilst the (secondary) road and weather parameters depend only on the respective primary model, the traffic ones are determined by the road type and season simultaneously. Figure and text borrowed from [10].

The set of parameters included in the sOC classification can be described mathematically as the set of parameters OC_s in equation (2-1), where OC stands for Operating Cycle and subscript s refers to stochastic.

$$OC_s = \{R_s, W_s, T_s, M_s\} \tag{2-1}$$

Also worth noting, the models and parameters of the sOC format have been introduced by Pettersson, Johannesson, et al. (2019) [24] with valuable contributions from Luigi Romano. Specifically, the weather and traffic models.

2.2.1 Primary models

There exist two primary models to this day, Road type and Season. Road type is determined by the speed limit and there exist three different road types currently. Those are, **Uban**, **Rural** and **Highway.** The primary model for Season is described by **Winter**, **Spring**, **Summer** and **Autumn**. Each secondary model inherits some of their stochastic parameters from the Primary models and is described in the subsequent Sections 2.2.2, 2.2.3 and 2.2.4.

2.2.2 Secondary road models

This Section presents the currently available stochastic models for modelling roads in the OC format.

2.2.2.1 Stop signs, giveaway signs, speed bumps & traffic lights

The occurrence of stop signs, giveaway signs, speed bumps and traffic lights is modelled in one dimension, location. These entities behave as discrete events that are scattered randomly between the start and end of the mission i.e, the sign location is a random variable X. Also, the sign probability is independent of previous signs i.e., the model fulfils the Markov property. An easy model with these characteristics is the Marked Poisson process, see equation (2-2). A Marked Poisson process does only require the sign intensity λ_s to be known, where the sign intensity is the rate of signs with respect to distance. Thus, the only dependency in determining the sign probability given a specific link is the link length.

$$X_{k+1} - X_k \sim \mathcal{E}(\lambda_s) \tag{2-2}$$

In [24] the authors recommended the use of a Uniform distribution to model the standstill time and the recommended speed. The uniform distributions are bounded by (t_{min}, t_{max}) and (v_{min}, v_{max}) respectively.

$$T_k \sim u(t_{min}, t_{max}) \tag{2-3}$$

$$V_k \sim u(v_{min}, v_{max}) \tag{2-4}$$

For giveaway signs, speed bumps and traffic lights, all five parameters are required for a full description. Those parameters are standstill time bounds (t_{min}, t_{max}), recommended speed bunds (v_{min}, v_{max}) and intensity λ_s. Stop signs are preferably described by standstill time bounds and intensity since the recommended speed should be zero in all instances.

2.2.2.2 Speed limits and ground type

The speed signs are assumed to be located at random positions and are therefore treated as a random process $V = V(x)$. A restriction for speed limits is that they can only take a value from the set $S_V = \{v_1, \dots, v_n\}$. Also, a greater part of the information regarding the next speed limit is contained within the current speed limit. Thus, Speed limits might be modelled as a Markov chain, see equation (2-5).

$$P\left(V_{k+1} = v_{i,k+1} \middle| V_1 = v_i, 1, \dots, V_k = v_i, k\right) \approx P\left(V_{k+1} = v_{i,k+1} \middle| V_k = v_i, k\right) \tag{2-5}$$

The Markov probability matrix is defined as $P_V \in \mathbb{R}^{n_v \times n_v}$ where each entry is the probability of transitioning from state i to state j. Assuming no self-transitions, all the diagonal elements are of zero probability. The other entries take the value according to equation (2-6), where f_{Vij} is the number of transitions from state i to state j.

$$p_{Vij} = \frac{f_{Vij}}{\sum_{j=1}^{n_v} f_{Vij}} \qquad \text{2-6}$$

The sign location is modelled as a set of Poisson processes, see equation (2-2). However, speed signs are not defined as a binary event, they can take all the states of S_V and does therefore require n_v number of intensities λ. Instead of representing the location of the speed signs as intensities, the writer chooses to define the mean length of a speed limit L_{mi} which is the inverse of the intensity λ. Given all, the whole model is fully parameterized by the set of variables $\{f_{vij}, L_j\}$ given $i, j = 1, \dots, n_v$.

2.2.2.3 Topography

The road, partitioned into small segments (links), has a road grade assigned to each of the links. Treating the road grade as a random variable $\{Y_k\}$ for each link k, an autoregressive model of order 1 can be used to model the grade, see equation (2-7).

$$Y_k = \phi_Y Y_{k-1} + e_{Y,k}, \qquad e_{Y,k} \sim \mathcal{N}(0, \sigma_{eY}^2) \qquad \text{2-7}$$

Here, ϕ_Y is the parameter of the model which can be interpreted as the memory of the previous link. The parameter is the factor that tells how much of the previous links' road grade is to be inherited from the current link. The parameter can preferably be rewritten in terms of the hill length L_h, see equation (2-8).

$$L_h = \frac{4\pi}{\pi - 2arcsin(\phi_Y)} L_s \qquad \text{2-8}$$

The error variance σ_{eY}^2 models deviations around the inherited value from the previous link. It can be expressed as the road grade variance, see equation (2-9).

$$\sigma_Y^2 = \frac{\sigma_{eY}^2}{1 - \phi_Y^2} \qquad \text{2-9}$$

The set of parameters $\{L_h, \sigma_Y^2\}$ is enough to model topography.

2.2.2.4 Curviness

Curvature is modelled by three parameters $\{X_k, C_k, L_k\}$. The location X_k modelled by a marked Poisson process, the curvature C_k modelled as a modified log-normal distribution and the curve length L_k modelled as a log-normal distribution. The location model is the same one described in Section 2.2.2.1. The Curvature modified log-normal distribution is defined by equation (2-10).

$$R' = 1/C - r_{turn}, \qquad log\ R' \sim \mathcal{N}(\mu_C, \sigma_C^2) \qquad \text{2-10}$$

Here, r_{turn} is the minimum curvature radius, μ_C is the mean of the log-normal distributed variable R' and σ_C^2 is the variance of the same variable. The curve length L is modelled using a log-normal distribution defined by the mean and variance μ_L, σ_L^2, see equation (2-11).

$$log\ L \sim \mathcal{N}(\mu_L, \sigma_L^2) \tag{2-11}$$

The stochastic model for curviness is therefore fully parameterized by the set of six parameters $\{\lambda_C, \mu_C, \sigma_C^2, r_{radius}, \mu_L, \sigma_L^2\}$.

2.2.2.5 Road roughness

The model for road roughness is not treated here and the reader is referred to Johannesson, Podgórski and Rychlik (2016) [19] for additional details.

2.2.3 Secondary weather models

Modelling weather is done under the assumption that weather properties remain approximately constant in space. The secondary weather models inherit some of their parameter values from the primary weather model. Depending on the choice of Primary model, a different set of parameters are retrieved.

2.2.3.1 Air temperature and relative humidity

Air temperature and relative humidity are assumed to be a composition of a deterministic variable and a stochastic variable. The deterministic term includes the yearly mean value $\{\mu_T, \mu_\Psi\}$, the annual trends $\{T_y sin\left(\omega_y d_y[t] + \varphi_{T_y}\right), \Psi_y sin\left(\omega_y d_y[t] + \varphi_{\Psi_y}\right)\}$ and the daily trends $\{T_d sin(\omega_d d_d[t] + \varphi_{T_d}), \Psi_d sin(\omega_d d_d[t] + \varphi_{\Psi_d})\}$, see equations (2-12) and (2-13).

$$T_{air,k} = \mu_T + T_d sin(\omega_d d_d[t] + \varphi_{T_d}) + T_y sin\left(\omega_y d_y[t] + \varphi_{T_y}\right) + \tilde{T}_k \tag{2-12}$$

$$\Psi_{air,k} = \mu_\Psi + \Psi_d sin(\omega_d d_d[t] + \varphi_{\Psi_d}) + \Psi_y sin\left(\omega_y d_y[t] + \varphi_{\Psi_y}\right) + \tilde{\Psi}_k \tag{2-13}$$

The annual frequency $\omega_y = 2\pi/365$ and the daily frequency $\omega_d = 2\pi/24$ treats the oscillating behaviour of weather. The time of the day $d_d[t]$ and the day of the year $d_y[t]$ are defined as:

$$d_d[t] = (t\ mod\ 24), d_y[t] = \left\lfloor \frac{t}{24} \right\rfloor \tag{2-14}$$

The phase angle φ handles the phase shift of daily and annual oscillation resulting from their sine wave model representation, where the subscript *d* represents day and *y* represents year. The set of sine waves amplitudes are $\{T_d, T_y, \Psi_d, \Psi_y\}$. Figure 2-2 shows the annual impact of temperature in Gothenburg. Given the figure, the set of annual temperature parameters T_y, φ_{T_y} in Gothenburg should be close to $8, -\frac{\pi}{2}$, see the green curve.

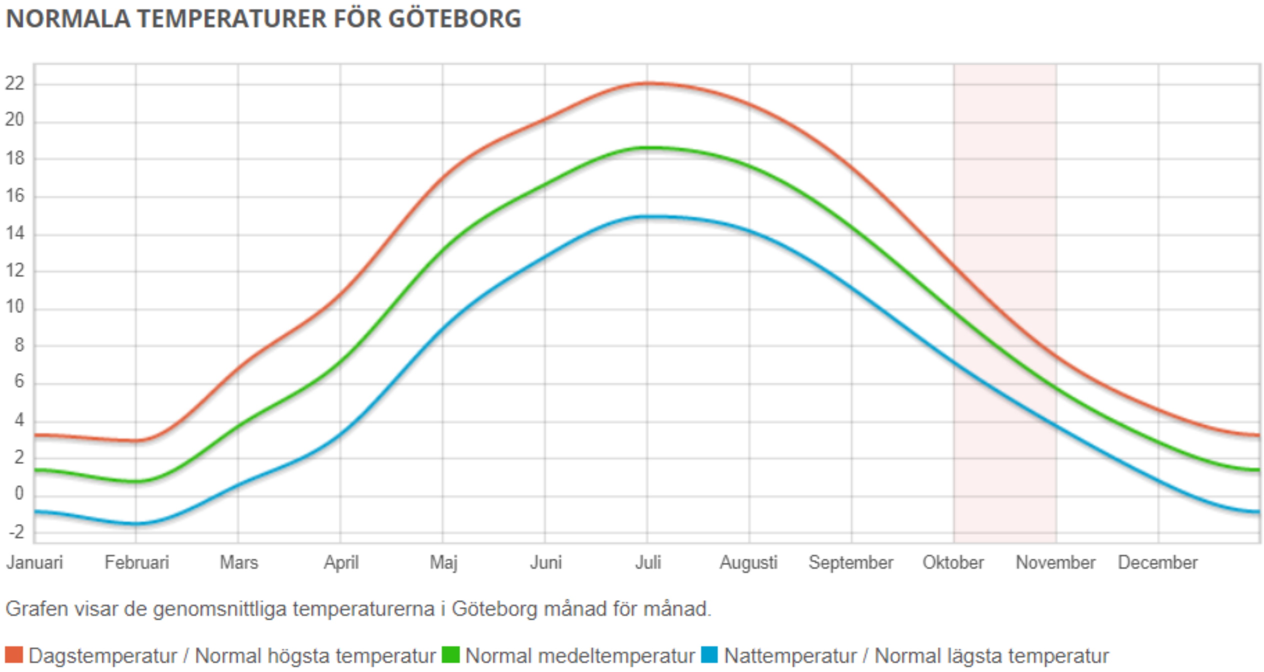

Figure 2-2. The monthly average temperature in Gothenburg. The phase angle seems to be about $\varphi = -\frac{\pi}{2}$. The figure is borrowed from [20].

The stochastic components $\{\tilde{T}_k, \tilde{\Psi}_k\}$ are modelled as an AR(1) process, see equations (2-15) and (2-16). For a more in-depth description of AR(1) processes, see Section 2.2.2.3 or [10].

$$\tilde{T}_k = \phi_T \tilde{T}_{k-1} + e_{T,k}, \qquad e_{T,k} \sim \mathcal{N}\left(0,\, \sigma_{eT}^2\right) \tag{2-15}$$

$$\tilde{\Psi}_k = \phi_\Psi \tilde{\Psi}_{k-1} + e_{\Psi,k}, \qquad e_{\Psi,k} \sim \mathcal{N}\left(0,\, \sigma_{e\Psi}^2\right) \tag{2-16}$$

The deterministic variables are calculated over a whole year and are independent of the seasonal setting. The stochastic parameters $\{\phi_T, \phi_\Psi, \sigma_{e_T}^2, \sigma_{e_\Psi}^2\}$ on the other hand, are not. The inherited value for the stochastic parameters does differ with the season.

2.2.3.2 Atmospheric pressure

The model for atmospheric pressure used is an ARIMA(p,d,q) process, see equation (2-17), where p is the model order of the AR(p) component, d is the model order of the integrating component I(d) and q are the size of the moving average window MA(q).

$$\phi_P(L)(1-L)^d P_{air,k} = c_P + \theta_P(L) e_{P,k}, \qquad e_{P,k} \sim \mathcal{N}\left(0,\, \sigma_{eP}^2\right) \tag{2-17}$$

The Autoregressive lag polynomial $\phi_P(L)$ is a function of the lag operator L. The rest of the parameters are the integrational component $I(d) = (1-L)^d$, the moving average function $\theta_P(L)$, the time series $P_{air,k}$, the drift c_P and the previous errors $e_{P,k}$.

The atmospheric pressure model is therefore fully parameterized by the set of four parameters $\{c_P,\ \phi_P(L),\ \theta_P(L),\ \sigma_{e_P}^2\}$

2.2.3.3 Precipitation

Precipitation is modelled in a two-step process. First, the occurrence of $H_{p,k}$ events are simulated and then a suitable probability density function is fitted to the intensity $\Lambda_{p,k}$ which is the amount of precipitation. A Markov chain with a fixed interval length is used to model the occurrence. The discrete random variable $H_{p,k}$ is allowed to take two states, *wet* and *dry*.

$$P\left(H_{p,k} = h_{p,k} \middle| H_{p,1} = h_{p,1}, H_{p,2} = h_{p,2}, \dots, H_{p,k-1} = h_{p,k-1}\right) \approx P\left(H_{p,k} = h_{p,k} \middle| H_{p,k-1} = h_{p,k-1}\right) \tag{2-18}$$

Since there are only two states, only two equations are required to fully characterize the model. The author chooses to parameterize the two entries of the anti-diagonal, see equation (2-19).

$$p_{H12} = 1 - p_{H11}, \qquad p_{H21} = 1 - p_{H22} \tag{2-19}$$

The self-transitions can easily be calculated from equation (2-20). Given this, the anti-diagonal is now known.

$$P_{H11} = f_{H11}/(f_{H11} + f_{H12}) \tag{2-20}$$

When a wet event occurs, a Gamma distribution is used to model the intensity of precipitation, see equation (2-21).

$$\Lambda_{p,k} \sim Ga\left(\alpha_{\Lambda_p}, \beta_{\Lambda_p}\right) \tag{2-21}$$

Precipitation is fully parameterized by the set of parameters $\{\alpha_{\Lambda_p}, \beta_{\Lambda_p}, f_{Hij}\}$.

2.2.3.4 Wind speed and direction

Wind speed and wind direction exhibit a strong correlation. Therefore, the model used has to portray the mutual dependencies. One of the simplest models that fulfils our requirements is the VAR model. It is an extension of an AR model that couples multiple random variables, see equation (2-22).

$$\mathbf{\Phi}_w(L)\, \mathbf{Y}_{w,k} = c_w + e_{w,k} \tag{2-22}$$

The vector $\mathbf{Y}_{w,k} = [V_{v,k}, \Theta_{w,k}]$ consists of the wind speed and the wind direction. The rest of the parameters are, the constant offset $c_w \in R^2$, the vector of normally distributed innovations $e_{w,k} \in \mathbb{R}^2$ with the covariance matrix $\sum e_{w,k} \in \mathbb{R}^{2\times 2}$ and finally the matrix operator $\mathbf{\Phi}_w(L)$. The matrix operator is defined by equation (2-23).

$$\mathbf{\Phi}_w(L) = \mathbf{I} - \sum_{j=1}^{p} \mathbf{\Phi}_{wj}\, L^j \tag{2-23}$$

The model is fully parameterized by the set of variables $\{\mu_{\Theta_w}, c_w, \Sigma_{e_w}, \Phi_{wj}\}$ for $j = 1, \ldots, p$.

2.2.4 Secondary traffic model

When modelling traffic, three main variables should be considered. Those are, the traffic density $\rho_t(x,t)$, the traffic speed $v_t(x,t)$ and the traffic flow $q_t(x,t) = \rho_t(s,t)v_t(x,t)$. Assuming stationary flow, we reduce the number of variables to two. In this case, traffic speed and traffic density are correlated and only one independent variable is needed to describe the state of traffic. The author chose traffic density. Traffic density is characterised by a diurnal component $\rho_d sin(\omega_d d_d[t] + \varphi_{\rho_d})$, a stochastic variable $\tilde{\rho}_k$ and the average traffic density μ_ρ given a specific road segment and season.

$$\rho_{t,k} = \mu_\rho + \rho_d sin(\omega_d d_d[t] + \varphi_{\rho_d}) + \tilde{\rho}_k \tag{2-24}$$

The model for traffic density is the same as for the secondary weather model Air temperature, see Section 2.2.3.1 apart from annual trends. Also, trivially the parameters do have another physical interpretation.
The vehicle speed v_e can be expressed, using Greenshields's fundamental diagram, see equation (2-25).

$$v_e(\rho_t(s,t)) = v_f\left(1 - \frac{\rho_t(s,t)}{\rho_c}\right) \tag{2-25}$$

Here, v_f represents the free-flow speed and ρ_c the critical density. The traffic model is fully parameterized by the set of six parameters $\{\mu_\rho, \rho_d, \varphi_{\rho_d}, \sigma^2_{e_\rho}, v_e, \rho_c\}$.

3 Model development

This chapter consists of four parts, Refinement and analysis, contributions to the Deterministic Operating cycle format, contributions to the Stochastic Operating cycle format, and a proposal of a Driver decision-making - Recharging concerning the accessibility of recharging stations.

3.1 Refinement and analysis of log vehicle data

This Section begins by Defining missions as a workday. After that, data refinement and analysis are performed for Mission Stops and Payload vehicle logs.

3.1.1 Defining missions as a workday

To define a mission as a workday, first one must define a workday. Given a set of data, recorded from a model FH2370 heavy vehicle one would like to define a typical workday. To do so, a time scheme of all recorded log files over a year is provided in Figure 3-1. Zooming in on the time scheme, reviles that the heavy vehicle is typically in operation during the daytime on weekdays. Since no logfile encountered was spanning the night hours, it is fair to define a mission as:

A mission is defined by all operations executed within a certain day.

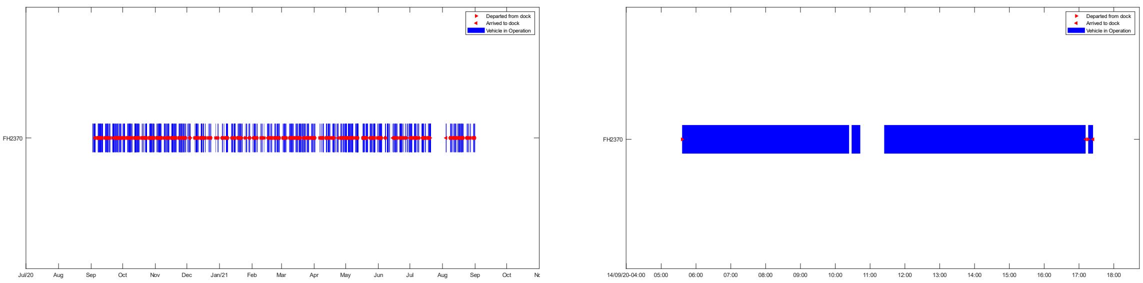

Figure 3-1. Start and end time of 1500 logfiles which constitute to one year of operation.

Given the mission definition, it is now easy to sort the log files into mission-specific folders. Mission 2020-09-14 presented in the right subfigure of Figure 3-1 consists of 4 logfiles, and we would like to concatenate those without losing valuable information. For example, it is important to identify all the mission stops since those are a part of the OC format. Out of curiosity, a small statistical analysis of all the missions is performed.

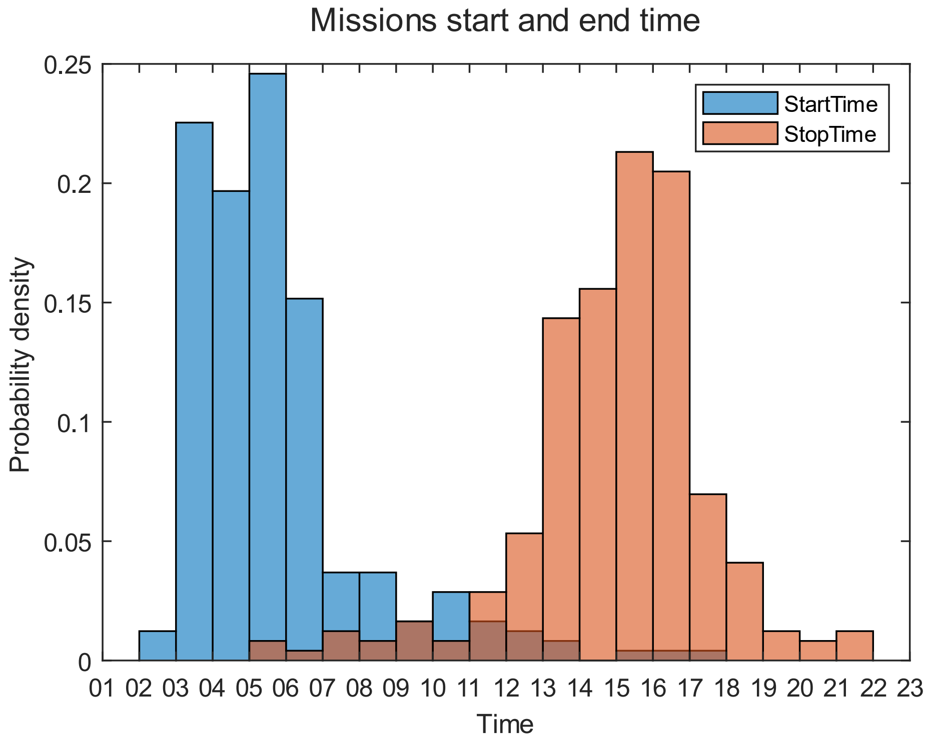

Figure 3-2. 112 Mission start and stop times represented in Histograms. 83% of all missions are started before 7 a.m. 93% of all missions are ended by 6 p.m.

From the probability histograms, one can conclude that most missions are relatively similar. The mission start is generally initiated before 7.00 and the mission is generally completed before 18.00. This allows for the postulation of the BEV to be fully recharged by every mission start. The assumption requires the dock to have a recharging point which seems like a fair assumption given that the haulage has a BEV.

3.1.2 Mission Stop

First, all mission stops initiated by one single heavy vehicle during one year of operation were collected. Then, the distribution of standstill time per mission is presented in a histogram together with a gamma distribution, see Figure 3-3.

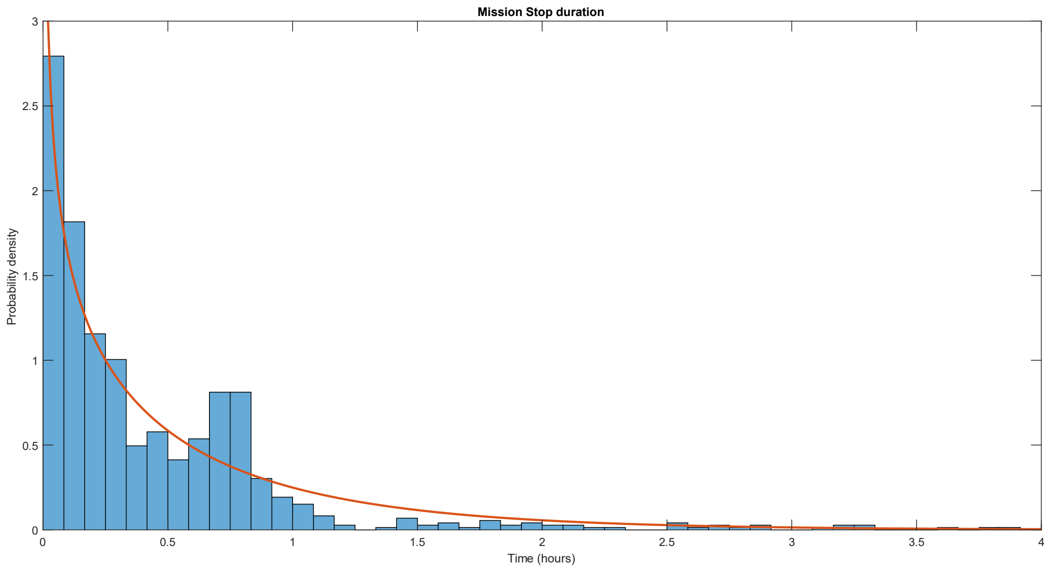

Figure 3-3. Mission stop durations. 90.9% of the Mission stops are of less than 1h in duration.

Given the small sample size (about 400 Mission stops), the risk of overfitting the data is present. Thus, the choice of distribution. The fit is decent except for around the 45-minute mark. It is reasonable to believe that the peak is due to the driver having a lunch break. A more sophisticated model could probably represent the mission stop better, such a model could be a bimodal distribution consisting of a normal distribution and a gamma distribution. The lunch break is normally distributed and every other stop is gamma distributed. This hypothesis of mine should preferably be further investigated before being perceived as accurate.

3.1.3 Payload

From the log files, a GCW estimate is available which is said to be noisy. The estimate is said to regularly deviate by up to 10% from the true mass signal but can under circumstances deviate by even more. The exact distribution and characteristics of the noise are unknown. Since the noise characteristics are unknown, a few assumptions regarding the true mass must be made. A reasonable starting point is to assume part-wise constant mass. Some change in mass is to be expected over time due to heavy rain, fuel usage and loss of material during travel. But it is fair to assume that such dependencies have a small impact on the total mass, and a change in mass is rather due to noise than actual mass change. An example GCW log is provided in Figure 3-4 for reference.

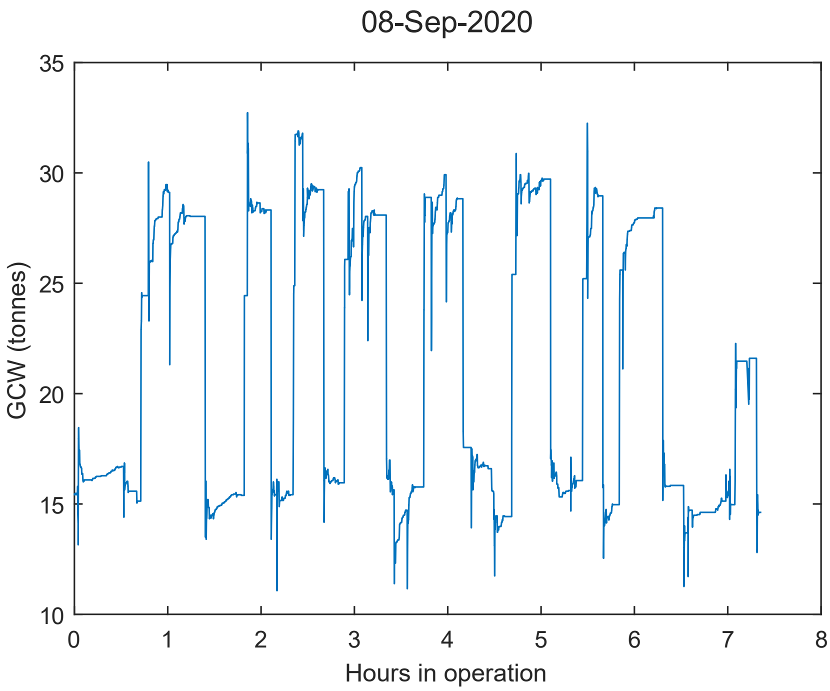

Figure 3-4. The logged GCW signal for Mission 8th of September 2020.

Since we don't know the true mass and its statistical properties, one must make a few justified assumptions. It is fair to assume the following:

1. Mass is piece-wise constant. A change in mass should be recorded over at least 10 minutes.
2. A change in mass is considered when a deviation of 10% or more, compared to recent mass values, is recorded. This implies that the weight of an unloaded heavy vehicle could deviate by about 1.5 tonnes and a fully loaded heavy vehicle by 6 tonnes.
3. Mass does always alternate between loaded and unloaded. The vehicle cannot be topped up when already partially loaded. Note that a trailer, loaded or unloaded, can be attached to the vehicle without a problem.
4. The driver loads and unloads all his goods instantaneously.

From these assumptions, it is fair to assume that the driver had nine load-on and nine load-off events during the day 8th of September 2020, see Figure 3-4.
To smoothen the GCW signal, first, let's start investigating if there are any patterns. A histogram built using all the GCW data points recorded over one year is presented in Figure 3-5.

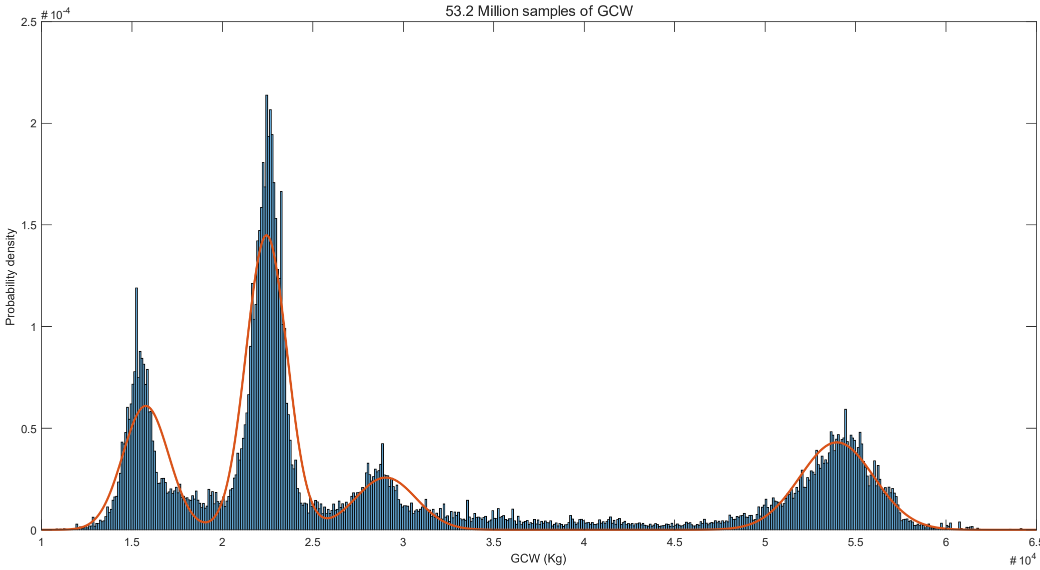

Figure 3-5. The histogram displays the distribution of all GCW data available. A multimodal distribution consisting of four normal distributions is fitted to the GCW data.

From Figure 3-5 one can identify that there are 4 different load cases. With this knowledge, one might view this as a classification problem. A first guess resulting from Figure 3-5, is that the classes might correlate with the fact that a trailer is connected or not. To investigate if that is the case or not, the GCW data is separated into two sets of data, **with trailer** and **without trailer**, see Figure 3-6.

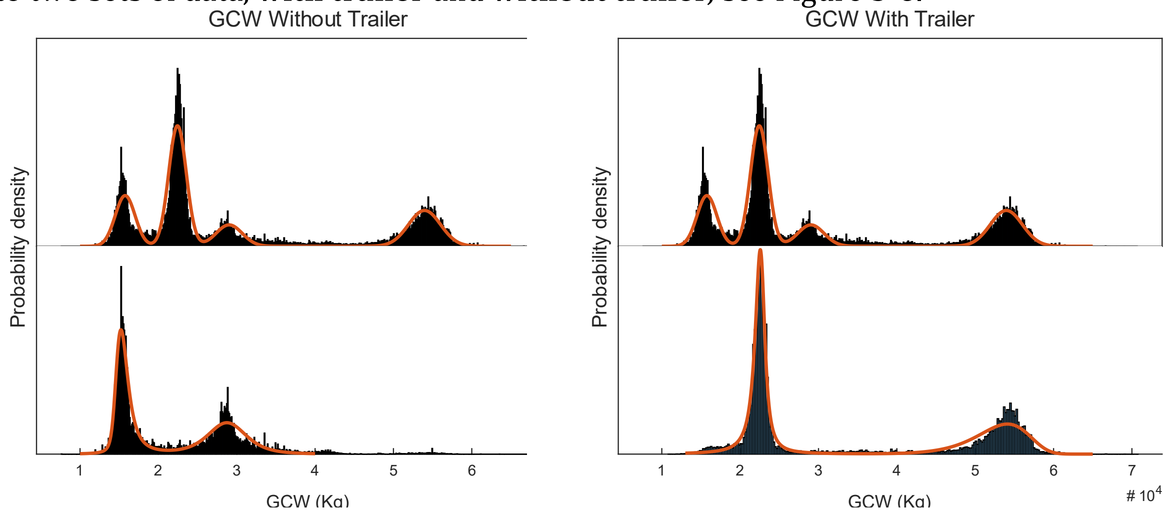

*Figure 3-6. The GCW data was split into two different sets of data, **with trailer** and **without trailer**. The upper histograms contain all the GCW data and the lower histograms are created using the two new sets of data. Two bimodal distributions are fitted to the data.*

From Figure 3-6, our first guess seems valid. The truck does operate under 4 different load cases. To ease the reading, each load case is assigned a state name according to Figure 3-7.

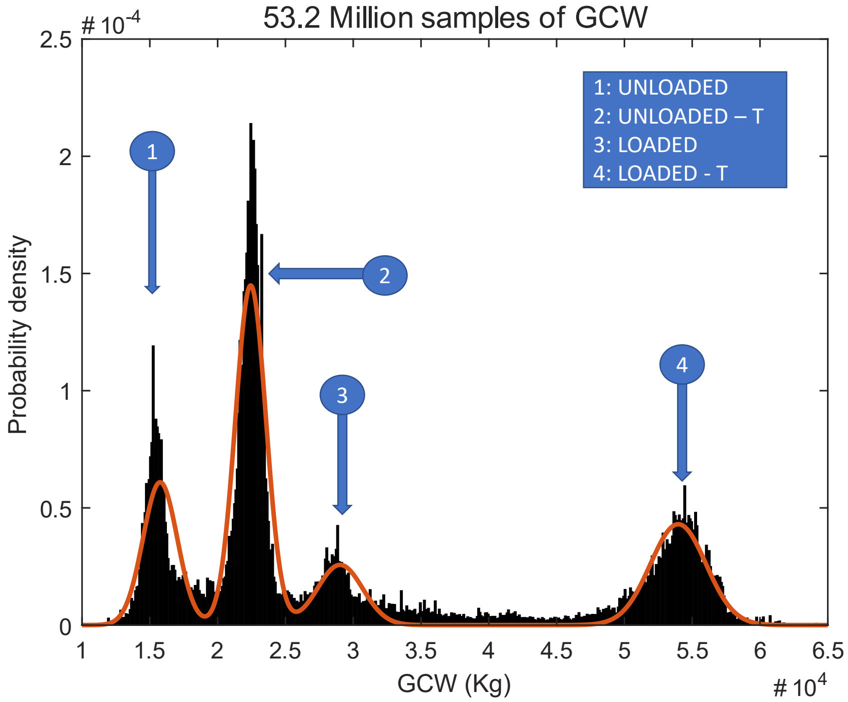

Figure 3-7. Schematic representation of states.

Now, to improve the fit, two bimodal distributions are fitted to the data. Their characteristic parameters are presented in Table 3-1. For this thesis, sample generation is of interest. Therefore, the complexity of the distributions is not considered. If one were to do more rigorous statistics, the author suggests using the normal distributions provided in Appendix A.1. The statistical parameters of interest for the payload estimation are the kerb weight and the trailer mean weight. The trailer's mean weight is defined as $\mu_t = \mu_{ut} - \mu_u$, where u is subscript for UNLOADED, ut is subscript for UNLOADED-T. Calculations resulted in a kerb weight of 16.22 tonnes and a trailer mean weight of 6.22 tonnes. For reference, the mean of a stable distribution is calculated using the formulae in equation (3-1).

$$\mu = \delta - \beta\gamma tan\left(\frac{\pi\alpha}{2}\right) \qquad 3\text{-}1$$

Table 3-1. Distribution characteristics of the four different load cases.

Payload Classifications	Distribution	α	β	γ	δ	μ	σ	ν
UNLOADED	Stable	1.309	0.647	623.02	15451.7	-	-	-
UNLOADED-T	Stable	1.137	-0.248	612.28	23134.7	-	-	-
LOADED	t-location-scale	-	-	-	-	28751	2555	3.90
LOADED-T	Weibull	54299.6	17.17	-	-	-	-	-

Viewing the problem as a classification problem, a threshold filter [12] should produce the desired result. A threshold filter is a classification filter which divides all the data into two new sets of data, the set of data that is above the threshold and the set of data that is below the threshold. The set of data that is below the threshold is assumed to be an unloaded heavy vehicle and everything above is assumed to be a loaded heavy vehicle. This type of filter is common practice within image processing but works perfectly for our use case as well.

But first, a transport mission is defined by the cargo rather than the vehicle. Enabling simulation using vehicle models with different kerb weights is one of the requirements of this model. Therefore, instead of estimating the GCW, the kerb weight is removed from the signal resulting in the Payload signal. This implies a shift in the x-axis of 16.22 tonnes in Figure 3-5, Figure 3-6 and Figure 3-7.
Now, given that we have access to the trailer-connected signal, it is possible to set a variable threshold. The variable threshold is discrete and can take two values, 3.5 and 10.5 tonnes. The threshold values are a result of the statistical analysis of the GCW data, where the threshold value should be somewhere between Unloaded and loaded. Without a trailer, this would imply 3.5 tonnes and with a trailer 10.5 tonnes.

$$T = \begin{cases} 3.5\ tonnes, & if\ no\ trailer\ connected \\ 10.5\ tonnes, & if\ trailer\ connceted \end{cases} \tag{3-2}$$

Given a specific mission, an example threshold is presented in Figure 3-8, where the red dashed line represents the variable threshold, see the upper subplot. The middle subplot is the product of the variable threshold, where 1 indicates above the threshold and 0 indicates below the threshold. The lower subplot is the filtered Payload signal.

Assuming that variations in the states UNLOADED and UNLOADED-T are due to noise, a constant value is assigned for segments of the signal being below the threshold. That value is 0 kg for UNLOADED and 6.22 (tare trailer weight) for UNLOADED-T. In contrast, the states LOADED and LOADED-T is allowed to vary since those are presumed to be caused by variations in load rather than noise.

Investigating several missions, it seems like the mass measurement is converging overdamped i.e., it does rarely overshoot. Therefore, the mass value assigned for parts of the signal that is above the threshold is the mean of the 10% max mass values registered over that part of the signal.

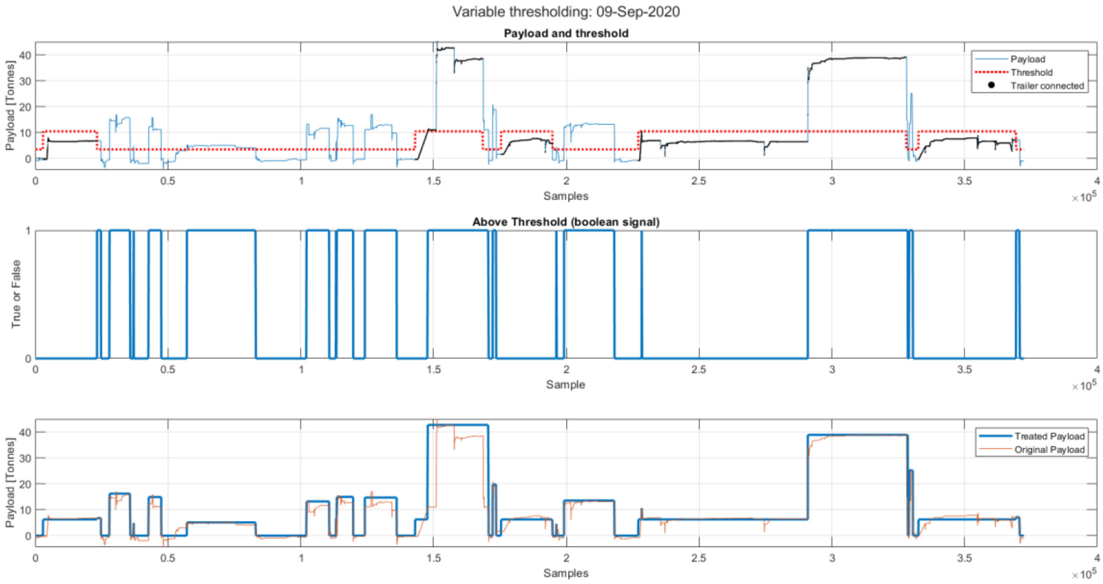

Figure 3-8. Variable threshold, logical threshold signal and resulting payload signal. The signal is sampled at a constant frequency of 10 Herz.

As one might notice, the signal does already look credible except for a few spikes in the signal. Those spikes are a huge problem though. Due to VehProp relying on the assumption of constant mass during travel, a mass change requires the driver to make a stop. With this in mind, it is important to not have an excessive amount of mass changes since this will result in an alteration of the transport mission. Therefore, a spike filter is treating the payload signal as well as the threshold signal, see Section A for the definition of a spike filter. A spike filter works as it counts the number of consecutive times a certain value is received. If the number of consecutive times is less than a certain value, it is considered a spike and the opposite value is assigned to the spikes. Two types of spikes must be treated, in this thesis, they will be referred to as drop-spike and peak-spike. A drop-spike is defined as a small segment of signal that is recognised as being under the threshold. The opposite applies to a peak-spike. An example of peak-spikes can be seen in Figure 3-8 around sample $1.7 \cdot 10^5$. An example of a drop-spike can be seen around sample $1.15 \cdot 10^5$. Removing the peak-spikes results in Figure 3-9.

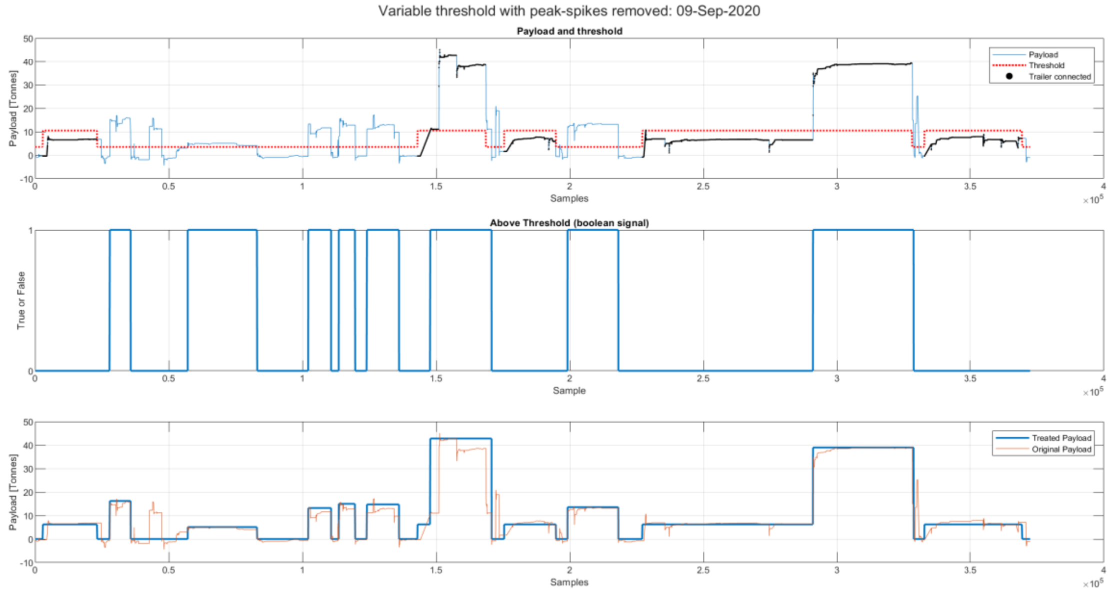

Figure 3-9. Variable threshold with peak-spikes removed.

The peak-spike filter removed all the spikes but it did also remove a suspicious spike just before sample $0.5 \cdot 10^5$. The spike is about 5000 samples in width and the spike filters consider a spike to be six thousand or fewer samples in width and does therefore remove that spike. One can argue that this should not have been considered a spike but given the assumption of partwise constant mass for 10 minutes i.e., 6000 samples with 10 Hz update frequency, it is considered a spike. Now, it's time to remove the drop spikes.

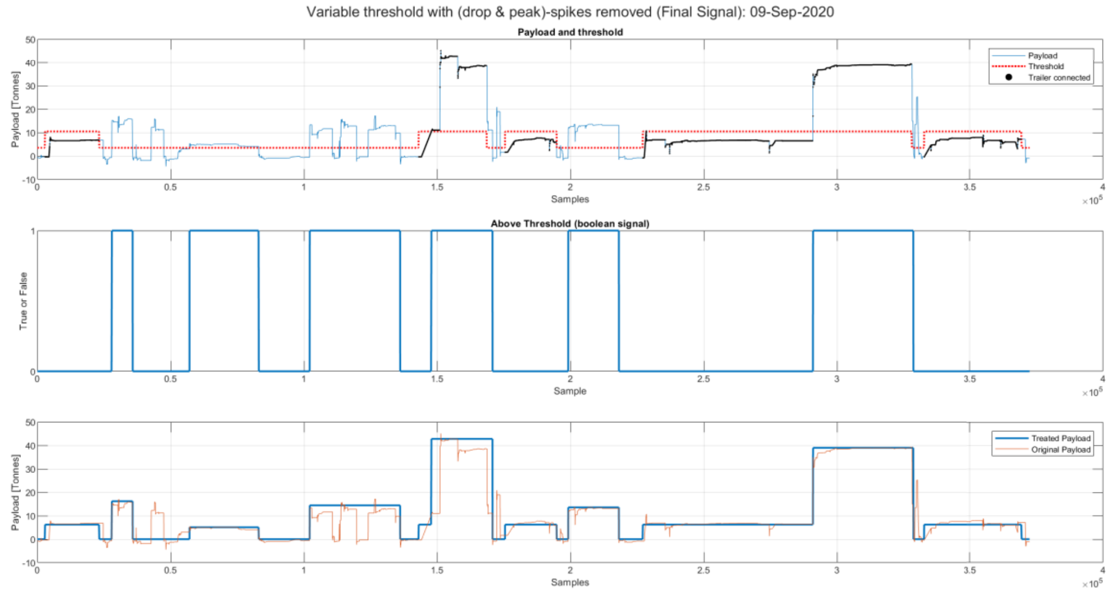

Figure 3-10. Final Payload signal.

Just as for the peak-spikes, a suspicious drop-spike was removed at sample $1 \cdot 10^5$ in Figure 3-10. If one does not agree with these spikes being removed, one should simply change the spike filter width that is set to 6000 consecutive samples.

3.2 Deterministic Operating cycle

This Section describes the contributions this study delivers to the dOC format.

3.2.1 EV-Recharging dOC model

The model for EV-Recharging purposed in this thesis quantifies a recharging event, in terms of energy acquired, but also enables smart driving behaviour. To do so, every Ev-Recharging station along the driven path is modelled rather than the power input as is purposed in P. Pettersson [21].

The deterministic model consists of a set of six variables, $\{X_k, P_k, T_k, \mu_k, \lambda_k, C_k\}$ for $k = 1, \ldots, n$ where n is the number of Recharging stations along the route. The distance X_k is the one-dimensional location of the recharging stations. Recharging stations are generally not encountered along a driven trace, but rather in close proximity to the trace through a highway exit or similar. Somehow, one must map the recharging stations' 2d coordinate position to the Operating Cycles' one-dimensional position, distance. A first solution to this is to assume that recharging stations are located along the mission path. Given that the distance to the recharging station is less than a set distance d_{max}, preferably the to-be driven distance (the exit distance), but an easier choice would be the linear distance, a charging station is said to be encountered.

The maximum available charging power P_k is measured in kW and is the station-specific max power output. Connector type T_k can take an integer value represented in equation (3-3), where each integer maps to a specific connector type. The connector types modelled are those available in Europe today [16].

$$T_k = \begin{cases} 1, & if\ Type\ 2 - Mennekes \\ 2, & if\ CCS/Combo\ 2 \\ 3, & if\ Other\ connector \end{cases} \tag{3-3}$$

The AFID directive 2019/94/EU requires every charging point to include either a type two or a CSS connector. Before the directive, charging points with other connectors were built and some of those remain. To limit the list of connectors, only the most prevalent ones are listed. Also worth noting, is that DC charging (CCS/Combo 2) is typically preferred since it allows for a much larger power output, but the number of charging stations supporting DC charging is much sparser. Therefore, AC charging stations is to be included in the format.

The mean service time $1/\mu_k$ is the average time for which a connector is occupied. The mean arrival rate λ_k is the rate at which vehicles line up to charge. The mean service time and the mean arrival rate should preferably be described by two vectors, each with 24 entries, one for each hour. Assuming that the mean arrival rate is correlated with traffic density, it is reasonable to have an average arrival rate for each hour of the day, see Figure 3-11.

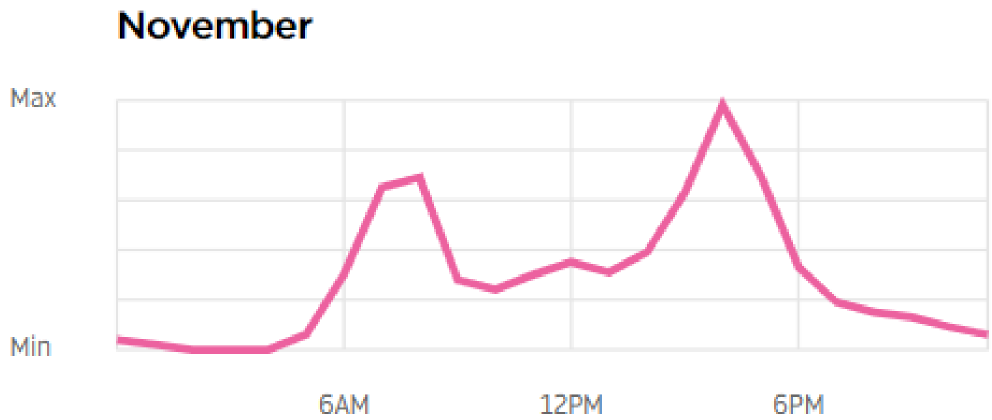

Figure 3-11. Average Traffic density in Gothenburg weekdays, November 2021 [17].

The maximum capacity C_k is the number of connectors a station is equipped with.

3.2.2 Payload and Mission Stop dOC models

No changes to the dOC models for Payload and mission stops have been required. The existing dOC model for mission stop requires the position and the standstill time. Payload is represented by the magnitude and position and is denoted Cargo weight in the dOC format.

3.3 Stochastic Operating cycle

This Section presents the contributions the present thesis has made to the sOC format.

3.3.1 Payload Stochastic model

The stochastic model for the payload is described by a combination of four processes, Distance travelled in state, Transitions between states, Payload magnitude of state and Initial state.

3.3.1.1 Distance travelled in states

First, the distance travelled in states is assumed to be equal for all states, i.e. no distinction between the distance travelled unloaded and loaded is made. This representation is a simplification that was made early in the project and a suggested future representation is presented under Section 4.3.2. Assuming that changes in states are best represented as randomly scattered events along the path, the distance travelled in states is modelled as a marked Poisson process, see APPENDIX A. A marked Poisson process does only require the mass change intensity λ_m to be known. Thus, the only dependency in determining the probability of an event given a specific link is the link length.

$$X_{k+1} - X_k \sim \mathcal{E}(\lambda_m) \tag{3-4}$$

3.3.1.2 Transitions between states

The second process is the transition between states. The probability of a certain state transition is modelled as a Markov chain, where a change in mass is assumed to have no self-transitions. This implies that our Markov matrix has no diagonal elements $P = \begin{pmatrix} 0 & \cdots & p_{j1} \\ \vdots & \ddots & \vdots \\ p_{i1} & \cdots & 0 \end{pmatrix}, \quad for\ i,j = 1,\dots 4$. Each entry p_{ij} represents the probability to move from state i to state j at the next event. The resulting Markov matrix P is presented in equation (3-5).

$$P = \begin{pmatrix} 0 & 0.8145 & 0.1855 & 0 \\ 0.2452 & 0 & 0.0044 & 0.7504 \\ 1 & 0 & 0 & 0 \\ 0.9461 & 0.0539 & 0 & 0 \end{pmatrix} \tag{3-5}$$

For a graphical representation, the Markov matrix is presented in Figure 3-12, where the colour of each arrow represents the probability of transition from state to state.

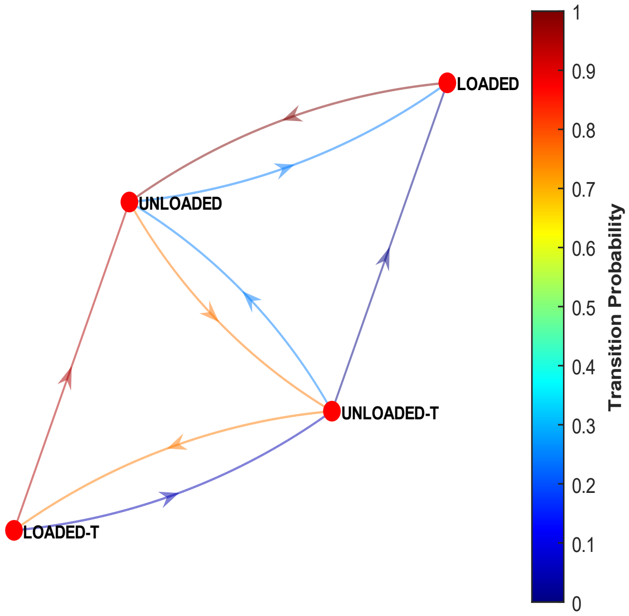

Figure 3-12. A Markov-chain directed graph. Each probability of transition is represented by the arrow colour.

Given the set of possible states $\{U, UT, L, LT\}$, a few interesting conclusions can be drawn. First, except for self-transitions, four transitions are of zero probability. Those are, $\{(L \to UT), (U \to LT), (L \to LT), (LT \to L)\}$. The first transition of the set is probably never perceived in reality. That state transition would imply that the truck gets unloaded and attaches a trailer at the same time. A more realistic transition is $(L \to U \to UT)$ which would have the probability of $1 \cdot 0.81 = 81\%$. The second transition of the set is also unreasonable, a more probable transition of events is $(U \to UT \to LT)$ which would have a probability of $0.81 \cdot 0.74 = 60\%$. The third and fourth transitions should be possible. But those state transitions can not be detected with the current filter implementation, see Section 3.1.3. These are transitions that do probably occur but go undetected because of the choice of filter, the threshold filter. Assuming those are intermediate transitions, the overall mass approximation remains relatively accurate. In other words, an improvement of the Payload smoother would result in an improvement of the Stochastic model. Given four zero probability transitions and no self-transitions, the set of stochastic parameters P summarizes to 9 parameters.

3.3.1.3 Payload magnitude of states

Now the third process is payload magnitude distributions. Given a certain state, the respective state mass is modelled by the four different distributions, characterized by their parameters presented in Table 3-1. An assumption regarding the states UNLOADED and UNLOADED-T is made. The variance around those states is presumed to be a product of noise rather than actual variation in the true signal. Therefore, those states can only take the constant values 0 and 6.22 tonnes respectively. But for the LOADED and LOADED-T, variations are assumed to be prevalent. The stochastic parameters needed to describe the Payload magnitude for state LOADED are $\{\mu, \sigma, \nu\}$, where μ is the location parameter, σ is the scale parameter and ν shape parameter. State LOADED-t requires the set of parameters $\{\alpha, \beta\}$, where α is the scale parameter and β is the shape parameter. Given all of this, the payload magnitude stochastic model requires the set of 5 parameters, $A = \{\mu, \sigma, \nu, \alpha, \beta\}$.

3.3.1.4 Initial state modelling

Lastly, the fourth process, initial state modelling. The Initial state is modelled by a generalized Bernoulli distribution with probabilities in equation (3-6).

$$P_{init}(X_i = x_i) = \begin{cases} 87.32\%, & if\, x_i = U \\ 9.27\%, & if\, x_i = U - T \\ 2.93\%, & if\, x_i = L \\ 0.49\%, & if\, x_i = L - T \end{cases} \qquad \text{3-6}$$

Probabilities are calculated from all the missions using equation (3-7), where f_i is the number of missions with initial state i.

$$\frac{f_i}{\sum_{i=1}^{4} f_i} \qquad \text{3-7}$$

3.3.1.5 Complete model

All four processes together describe the payload of a heavy vehicle. The stochastic parameters needed are the set of model parameters $\{\lambda, P, A, P_{init}\}$ which adds up to nineteen parameters.

3.3.2 Mission stop stochastic model

A mission stop is defined as a stop that requires the engine to be turned off. The deterministic model for mission stops requires two parameters, distance and standstill time. Given that we have no information on when and where a mission stop occurs, the occurrence of a mission stop is modelled as a Poisson process. This implies that the mission stops are scattered randomly over the whole trace. In contrast to the position of the mission stop, the standstill time could benefit from a data-driven approach using vehicle log data. In Section 3.1.2, standstill time is presumed to be a gamma process. The parameters (α, β) of the fitted gamma distribution are presented in equation (3-8), see Appendix A.6 for a rigorous explanation of gamma distributions.

$$X_k \sim \Gamma(0.6595, 0.8062) \qquad \text{3-8}$$

3.3.3 EV-Recharging stochastic modelling

This Section purposes a stochastic model for the EV-Recharging.

3.3.3.1 Location of EV-Recharging station

The stochastic model for EV-Recharging assumes charging stations to be located at random. Recharging stations scattered as a sequence of discrete events along a path described in one dimension can preferably be modelled by a marked Poisson process. A marked Poisson process requires one parameter, λ_p the rate of charging stations with respect to distance. Each mark represents a charging station which in turn has a set of characteristic parameters.

3.3.3.2 Maximum available charging power, connector type and capacity

The maximum available charging power P_k, the connector type T_k and capacity C_k are all modelled by a generalized Bernoulli distribution, see equation (3-9). They are all modelled with a uniform probability of $1/n$, mimicking a dice roll due to lack of information. A more advanced distribution would probably represent these stochastic variables better, but given the lack of information, the present thesis purpose an easy distribution for those variables.

$$P_k \sim f(x = i) = \frac{1}{n_p} \tag{3-9}$$

$$T_k \sim f(x = i) = \frac{1}{n_T} \tag{3-10}$$

$$C_k \sim f(x = i) = \frac{1}{n_C} \tag{3-11}$$

3.3.3.3 Average service and arrival rate

The average service rate μ and the average arrival rate λ are modelled by two normal distributions.

$$\mu_k \sim N\left(\mu_{\mu,n}, {\sigma_{\mu,n}}^2\right), \qquad Where\ \mu_k \neq 0 \tag{3-12}$$

$$\lambda_k \sim N\left(\mu_{\lambda,n}, {\sigma_{\lambda,n}}^2\right), \qquad Where\ \lambda_k \neq 0 \tag{3-13}$$

The mean and variance of the pdfs are yet to be known. A case study should preferably be conducted to get a better understanding. A possible provider of such data is VIRTA networks.

3.3.3.4 Complete model

In total, the set of eight parameters $\{\lambda_p, n_p, n_T, n_C, \mu_{\mu,n}, \sigma_{\mu,n}, \mu_{\lambda,n}, \sigma_{\lambda,n}\}$ fully parameterize the stochastic model for EV-Recharging.

3.4 Driver decision-making - Recharging

With the dOC definition of EV-Recharging, the driver can make recharging decisions concerning average waiting time W_q and average time spent in the system (waiting and charging) W_s to name a few. From queueing theory, an easy and intuitive model is constructed. The Kendall notation $(M/M/S)$: $(FCFS/\infty/\infty)$ is in this thesis purposed to model recharging stations. The inter-arrival rate and the rate of service are both modelled as Poisson processes. The number of service channels (charging points) is assumed to be 1 or more which is denoted as M in the equations below. The number of service channels is the same as the *Recharging station capacity* (C_k), described in Section 3.2.1, assuming that all the connectors are functional. A more detailed description of the Kendall notation is found in APPENDIX A. The expressions for W_s and W_q is displayed below in equation (3-16) and equation (3-18) respectively, where P_0 is the probability of no vehicles being present in the system, L_s is the average number of vehicles in the system and L_q is the average number of vehicles in the queue.

$$P_0 = \frac{1}{\left[\sum_{n=0}^{M-1} \frac{1}{n!}\left(\frac{\lambda}{\mu}\right)^n\right] + \frac{1}{M!}\left(\frac{\lambda}{\mu}\right)^M \frac{M\mu}{M\mu - \lambda}}, \qquad for\ M\mu > \lambda \tag{3-14}$$

$$L_s = \frac{\lambda\mu(\lambda/\mu)^M}{(M-1)!\,(M\mu-\lambda)^2} P_0 + \frac{\lambda}{\mu} \tag{3-15}$$

$$W_s = \frac{L_s}{\lambda} \tag{3-16}$$

$$L_q = L_s - \frac{\lambda}{\mu} \tag{3-17}$$

$$W_q = \frac{L_q}{\lambda} \tag{3-18}$$

Here, it is important to understand the difference between the average time in the system W_s and the simulated vehicles' average time in the system $W_{s,vehicle}$. The simulated vehicle is necessarily not properly represented by the average vehicle. Since we have information regarding the simulated vehicle it would be preposterous to not include that information in the model. The average simulated vehicle service time is described in equation (3-19), where $\mathrm{W_q}$ is a scalar, $\mathrm{E_{req}}$ is the driver-defined requested amount of recharge energy and $\mathrm{P_k}$ is the max power output from the recharging station.

$$W_{s,vehicle} = \mathrm{W_q} + \frac{\mathrm{E_{req}}}{\mathrm{P_k}} \tag{3-19}$$

Trivially, one would like to minimise the variable $W_{s,driver}$. Fixating the energy request $\mathrm{E_{req}}$ to an arbitrary fraction of the battery capacity, let's say 1/3. Using range prediction, it is possible to locate all the stations that are along our trace before the battery *state of charge* (Soc) level is estimated to be below 20%. Now, calculate the estimated time in the system for the simulated vehicle and choose the recharging station with the smallest $W_{s,vehicle}$. Do the same calculations recursively over the whole simulation. This is a neat and easy model that should and could easily be further developed. For example, one could introduce constraints on charging time or waiting time. Also, the driver does probably prefer time in service over time in a queue since service enables the driver to exit the vehicle.

4 Case studies

This chapter consists of three parts, a description of the Simulation environment, a Feasibility analysis of replacing an ICEV with a BEV and an analysis of the Framework delivery

4.1 Simulation environment

This Section consists of three parts, a description of the dOC parameters used, a list of Assumptions made, and two tables presenting Vehicle specifications for the logged vehicle and the BEV vehicle model.

4.1.1 dOC parameters

Even though models and data are available for the dOC models, the BEV Vehicle model does not make use of all the fields of the format. The supported fields are Mission and Road resulting in simulations being carried out with the dOC parameters presented in Table 4-1.

Table 4-1. dOC parameters used in simulations with VehProp.

	Description	Unit
Road:		
Topography:	Altitude	(m)
Legal speed:	Speed limit	(m/s)
Curvature:	Radius of circle segment	(1/100 meter)
Stop sign:	Standstill time	(s)
Speed bump:	Length, height, angle	(m, m, degree)
Traffic light:	Standstill time	(s)
Mission:		
Payload:	GCW – kerb weight = Payload	(kg)
EV-Recharging:	Power	(watt)
Power take off:	Time	(s)
Travel direction:	(1=forward, 0=reverse)	(boolean)
Mission Stop:	Standstill time (engine turned off)	(s)
Mission matrix:	Composition of Mission parameters	(Boolean, kg, watt, watt, Boolean, s)

4.1.2 Assumptions

A few assumptions regarding certain vehicle systems and dOC parameters are required to enable simulation. The assumptions made are those presented in the bullet list below.

- Every mission stop is seen as a recharging opportunity. As soon as the vehicle initiates a mission stop, recharging with 350kw is initialized. The purposed dOC model for EV-Recharging, see Section 3.2.1, is yet to be implemented. The dOC EV-Recharging format purposed can describe a more realistic recharging behaviour. Although to limit this study, implementation and evaluation of that model are yet to be produced.

- Recharging by regenerative braking is only limited by the battery charging limit which is 200 kW. It is reasonable to believe that the generators themselves have a power output limit that is not accounted for. Worth noting, the same saturation (200 kW) applies for the external EV-Recharging since it is a limitation of the vehicle battery.

- The VehProp BEV vehicle model is rather simple. Due to simplicity, some dynamics of the Operating Cycle format are lost. For example, there exists no traffic model or weather model. Also, some dynamics in the vehicle are simplified and biases are likely introduced, affecting energy consumption.

- Several signals are missing in the log and do therefore have to be estimated. To name a few:
  - PTO power signal
    - A Boolean On and off signal is available, but no power measure. Therefore, PTO power output is estimated to be a pulse with two kW magnitude. It is reasonable to believe that PTO Power output could be better estimated. Usually, one can measure the engine shaft power output (torque x angular velocity) during PTO usage. But due to uncertainties regarding the logged signal and to limit the project frame, no further study of this was conducted.
  - Stand still time while loading on/off the vehicle.
    - A study of loading times showed that 30 tonnes worth of soil takes about 150 seconds to be loaded using a single excavator. Assuming some time spill, a load event is estimated to take 300 seconds.
  - Speed bump dimensions
    - Brief market research was conducted. One world standard speedbump, consisting of a circle segment, named the watts hump typically has the dimensions 3.7 x 0.1 (width x height) [18]. Assuming the ramp is close to triangular, these bumps would have a slope of about 3.1 degrees. Given our imitated information regarding the specific speed bump encountered and the limited knowledge within the field, a harsher measure is used, a hump with dimensions 4.0x0.1 but with an angle of 4.3 degrees.

The takeaway from the assumptions made is that the simulation result will not represent the past perfect as always with simulations. Given the generous recharging modelling together with the lack of weather impact modelling, it is fair to assume that the simulation result will score higher in terms of success rate compared to what field studies would suggest. The analysis should therefore be treated as an upper limit to how well a BEV could perform, rather than how well it will perform using today's available technology.

4.1.3 Vehicle specifications

The vehicle logged during field tests is presented in Table 4-2.

*Table 4-2. Logged heavy-duty vehicle specifications. *Estimated from vehicle log data.*

Model:	Volvo FH16 750 hp, 8x4

Engine designation:	D16K 750 Step D, 16.1.1
Max revs:	2000 rpm
Max torque:	3550 Nm
Gearbox:	ATO3512F ASO-C
Kerb weight:	16 220 Kg*
WB wheelbase:	4300 mm

In table Table 4-3, the vehicle used in the simulation.

Table 4-3. Bev specifications.

Model:	Volvo FH Electric
Driveline:	2 electric motors
Battery capacity:	739.26 kWh
Max torque:	1898.7 Nm
Max Power:	510 kW
Kerb weight:	11042 Kg
WB wheelbase:	4370 mm

It is important to recognize the differences between the two vehicle models. Just from the vehicles, one should expect differences in energy consumption, driving behaviour etc. The logged vehicle is a much stronger and larger vehicle resulting in possibly more aggressive driving behaviour and larger energy consumption.

4.2 Feasibility analysis of replacing an ICEV with a BEV

This Section investigates the feasibility of replacing a specific heavy vehicle with a BEV.

4.2.1 Findings

A year's worth of dOCs meant that 159 missions were simulated. The feasibility of replacing the specific ICEV with the BEV without altering the transport mission is evaluated solely concerning battery capacity. No consideration of power limitations was taken. Missions that fail to be simulated are therefore not included in this analysis. If those missions fail due to power limitations or simulation environment errors is yet to be known. Therefore, an outlier rejection cell identifying failed missions is described by the list below, where subscript s and l represent simulation and log file respectively.

1. $\frac{|d_s - d_l|}{d_l} < 5\%$
2. $2 > \frac{t_s}{t_l} > 0.5$
3. $1.2 > \frac{\mathrm{E_s}}{\mathrm{E_l}} > 0.8$

A mission is deemed valid when all three arguments are passed as true. The numbers are, even though looking, not random. The first cell, where d is total mission distance driven, rejects simulations that have not completed the whole mission. This one is very strict compared to the other cells. If the distance does vary by more, one should question the degree of representation. The second argument, where t is the total time of the mission, is very loose. There are multiple reasons for time to vary e.g., differences in driving behaviour and idling. The window could be narrowed for longer missions, but for shorter missions idling can result in large differences. Therefore, a wider window is accepted. The third argument, where E is the total engine shaft energy output over a mission. All these arguments are wide enough to avoid removing any valid simulation results while remaining narrow enough to remove invalid simulation results. Some of these arguments could have narrower windows without problem, but there is no need to, hence no further tuning was initiated.

In the feasibility analysis, a mission is classified as successful if the DoD (depth of discharge) never surpass 70%. Accounting for battery degeneracy and voltage losses at low Soc levels, it is reasonable for a BEV to only deliver 70% of its maximum battery capacity. Given all, the maximum DoD during all missions is presented in Figure 4-1.

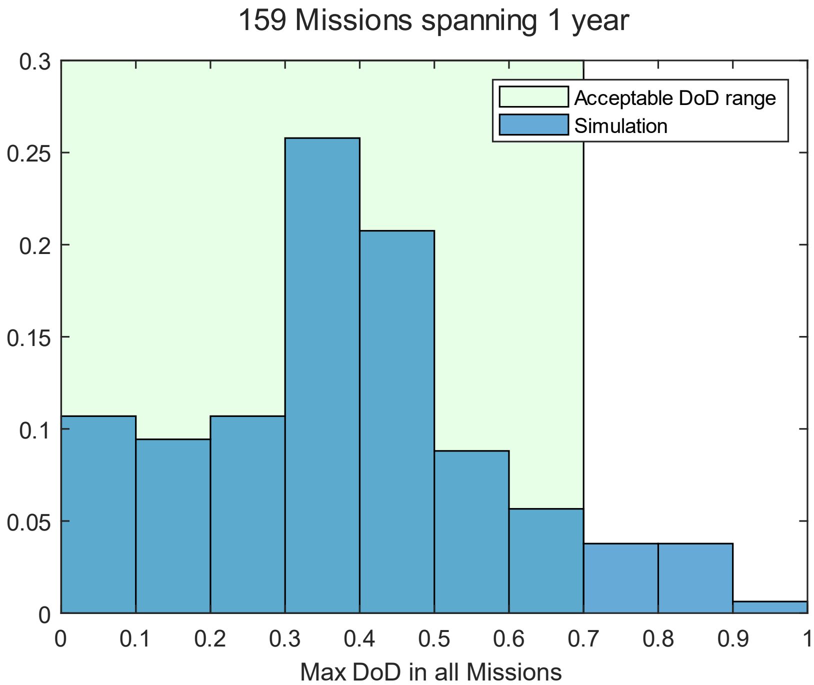

Figure 4-1. Bar plot of DoD normalized to sum 1. The Green area represents missions that are classified as successful. Missions outside the green area can not be completed without alteration in the transport mission.

The fraction of missions that cannot be completed without alteration in the transport mission is about 8 %. To highlight the sensitivity, if the acceptable DoD range instead shrinks to 0.56 the fraction of failed missions doubles to about 16%. That said, it is of the highest importance that the simulation result is accurate. This study shows, even though being very generous with recharging, that the BEV used in simulations cannot perform the same transport missions as an FH16 can do. About two transport missions per month cannot be completed without alteration. Trivially, the amount of alteration does differ from transport mission to transport mission. Studying the failed missions, an interesting aspect is revealed. A couple of the failed missions could be classified as successful if the driver were to initiate a stop and charge a bit earlier, see lower subfigure in Figure 4-2.

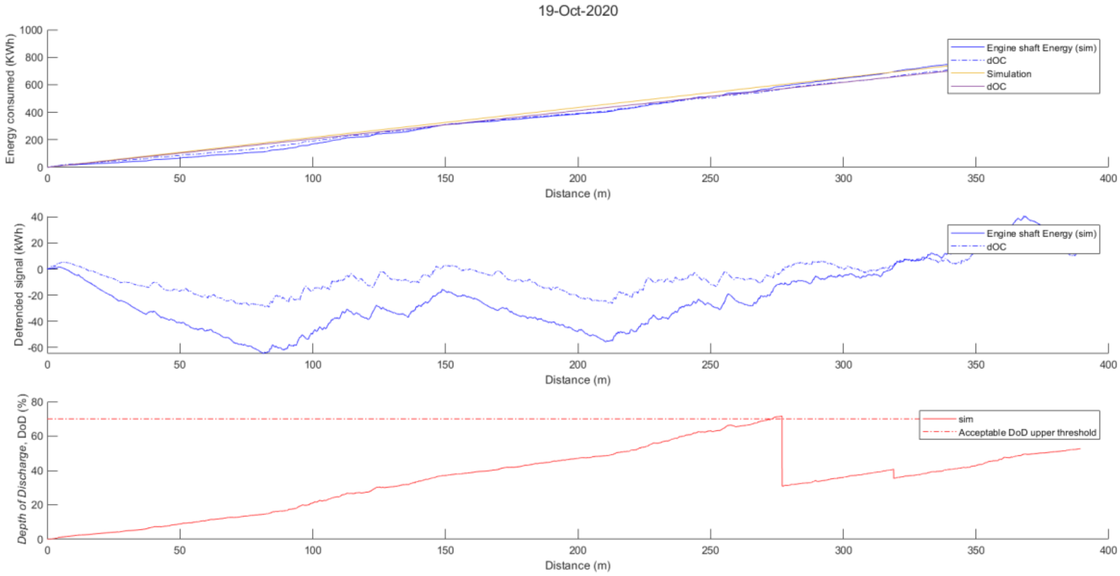

Figure 4-2. Mission 2020-Oct-19 energy comparison of simulation and log. The upper subplot presents the cumulative energy consumed over the whole mission and its linear trends. The middle subplot presents the deviations of cumulative energy consumed around the linear trend. The lower subplot presents the DoD level during simulation.

In Figure 4-2, the DoD just surpass 0.7 at about 275km. If the driver could make the same stop just a couple of km earlier, the mission would be classified as successful. Altering the transport mission like this might not be possible given that the driver must comply with delivery deadlines, lack of recharging stations, etc. But given flexible transport mission scheduling, it is possible to reduce the fraction of failed missions to 7% if a mission stop is allowed to be frontloaded. But then again, it is difficult to assess compliance in altering those transport missions. Also, given the generous recharging modelling, it is fair to assume that the transport missions would have to be even more frontloaded in reality compared to simulations.

4.3 Framework delivery

This Section evaluates the quality of the results presented in the previous Section and the stochastic models developed in Section 3.3.

4.3.1 Deterministic model evaluation

To verify the simulation environment as well as the dOC description, the engine shaft energy output is compared in Figure 4-3.

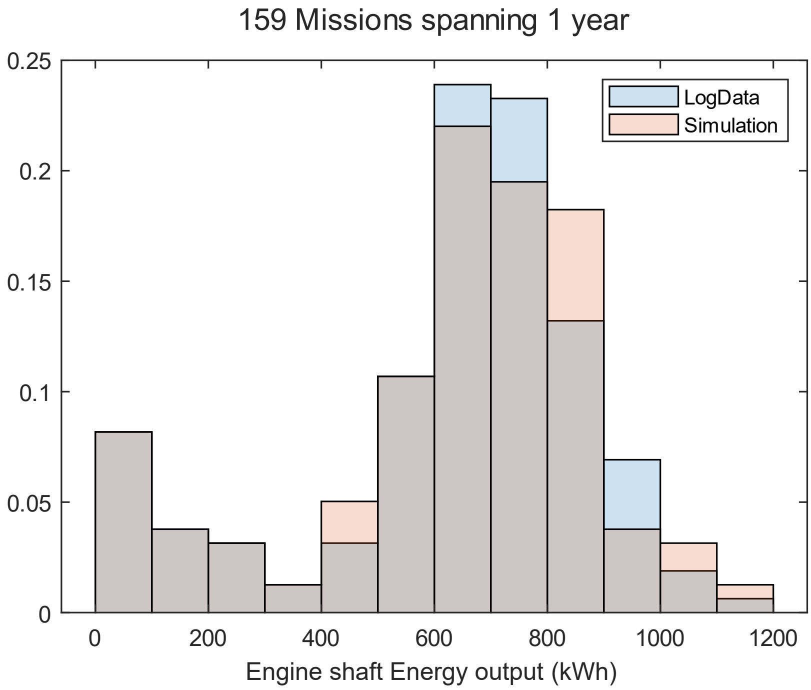

Figure 4-3. Comparison of total energy consumed during missions measured at engine shaft.

Given that we are comparing the engine shaft energy output, this result is very accurate. There are a couple of things that should vary between our simulated BEV compared to the logged FH16 vehicle.

- Friction in transmission.
- Rolling resistance.
- Weather impact on the vehicle.
- Driver behaviour.

To compare the simulation result with the log data, a line which minimizes the squared error is fitted to the energy consumption in simulation and in logging for every mission. The difference in slope of those lines is then collected and displayed in a histogram in Figure 4-4. The mean of the histogram represents the linear error that the simulation environment on average produce. Such bias could be caused by a misrepresentation of RRC, payload, etc.

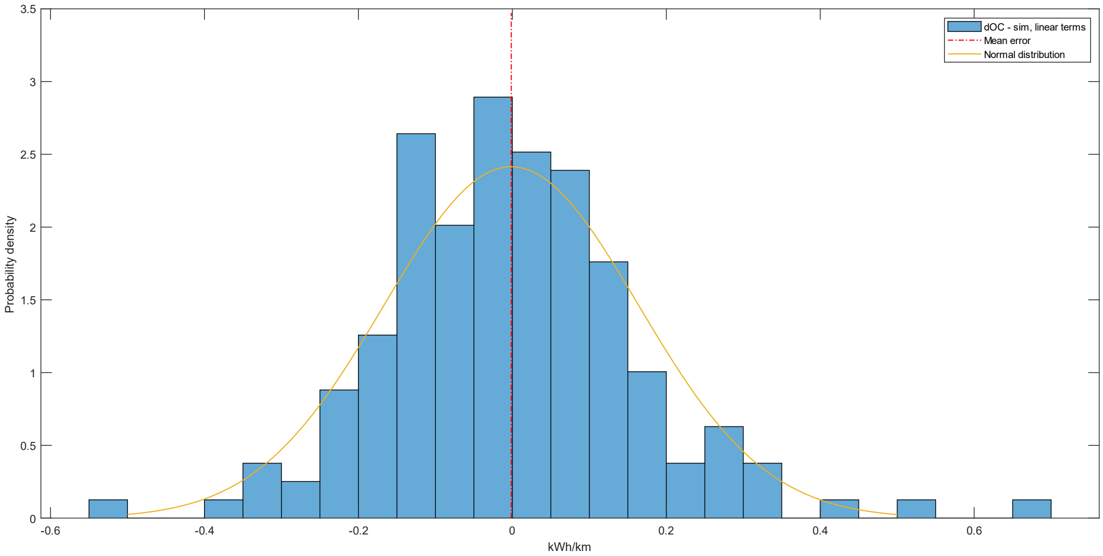

Figure 4-4. Comparison of linear terms. The x-axis represents the linear term offset when comparing simulation results to logged field data.

In Figure 4-4, one might notice that the linear error is close to normally distributed with a mean of zero. This implies that an arbitrary mission is expected to be simulated with zero linear bias in energy consumption compared to the log files.

Another factor affecting energy consumption is the total mission time and distance. Allowing a transport mission to extend the timeframe, gives the driver the possibility to drive more fuel efficiently resulting in unfair simulation results. In Figure 4-5, the error between the simulation and the log file is presented. The difference in total time seems to approximately be normally distributed with a mean of -0.2h and a variance of 1.

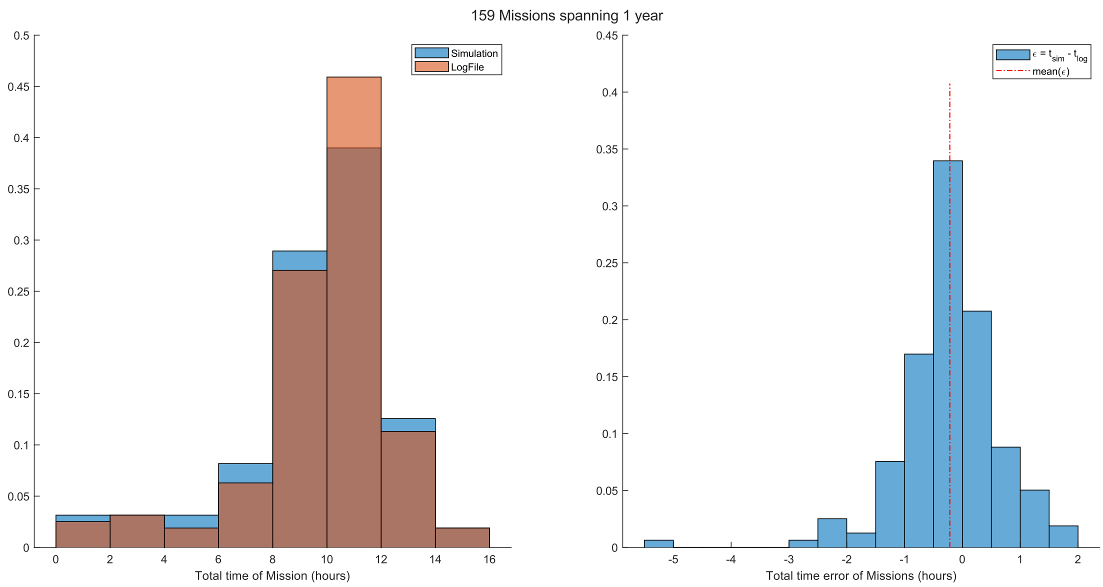

Figure 4-5. Comparison of total time per mission between logged vehicle data and simulation results.

Assuming missions are operated under a 10-hour timeframe, a deviation of up to 2 hours is quite large. It implies that the simulation environment does at instances finish a mission 20% faster/slower compared to the logged vehicle. The cause for

this is yet to be known but a list of the most likely reasons is provided in Section 5.2.
Now, the error in distance travelled is presented in Figure 4-6.

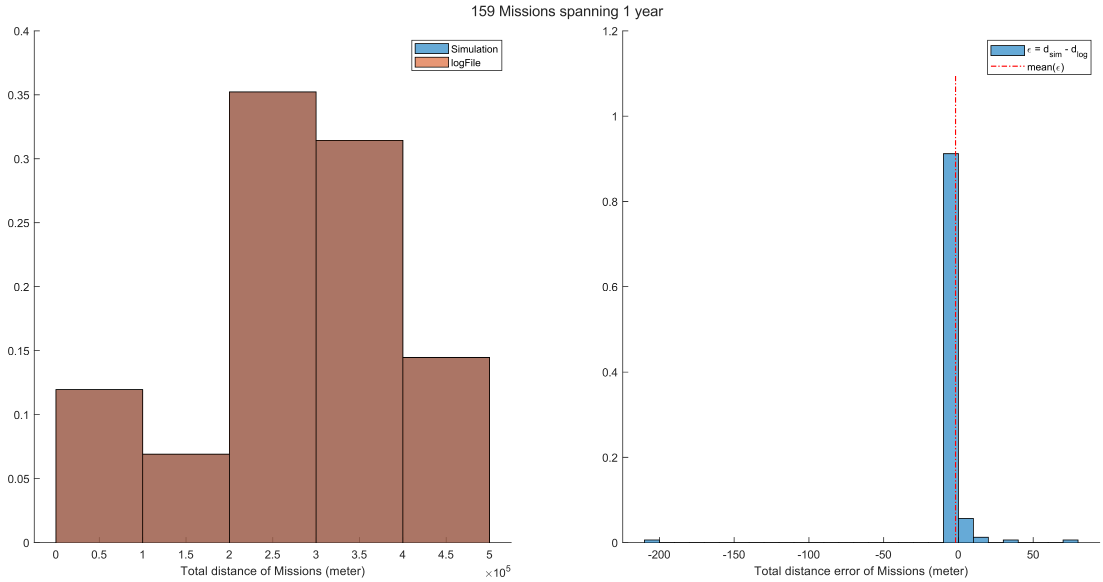

Figure 4-6. Comparison of total distance driven per mission between logged vehicle data and simulation results

The difference in total distance travelled is neglectable. A dozen meters is not impacting the overall energy consumption of missions operated for up to 500 km.

To further evaluate the format, A specific mission is analyzed to prove the concept. In Figure 4-7, the cumulative energy consumed is plotted against distance. To verify the shape, the linear trend in energy consumption is removed and the resulting signals are presented in the middle subplot. The DoD although interesting, is impossible to prove since we have no data to do so.

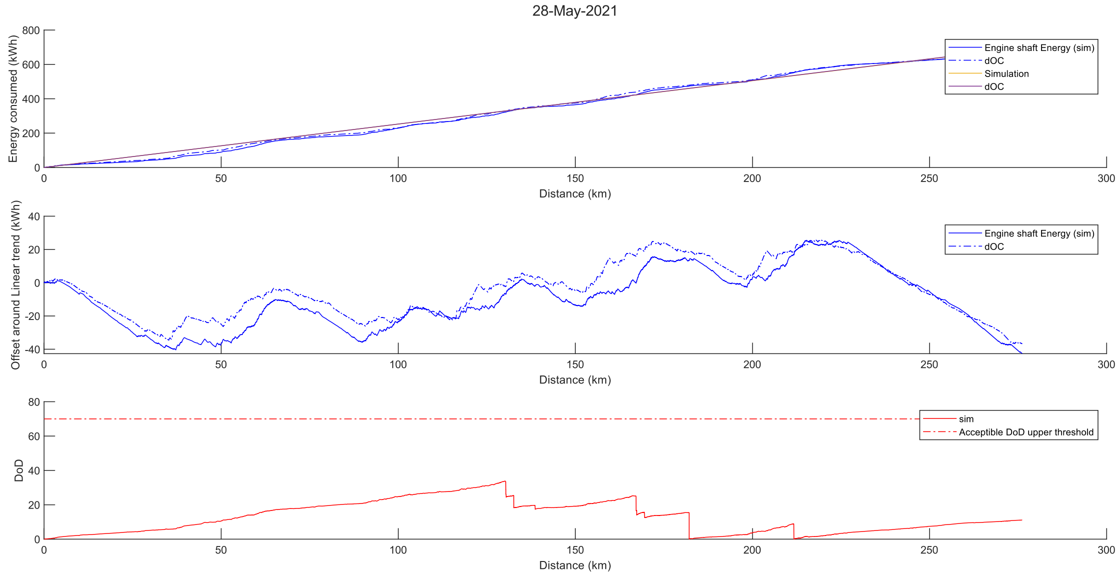

Figure 4-7. Mission 2021-May-28 energy comparison of simulation and log. The upper subplot presents the cumulative energy consumed over the whole mission and its linear trends. The middle subplot presents the deviations of cumulative energy consumed around the linear trend. The lower subplot presents the DoD level during simulation.

Except for the energy consumption, we should expect to have a similar speed profile. In *Figure 4-8*, the speed signal is presented. The upper subplot presents the measurement and the lower subplot the filtered measurement using a moving average filter. Here one might notice that the velocity profile of the field tests and simulations do compare quite well, indicating once again that the OC format is a good representation of a transport mission.

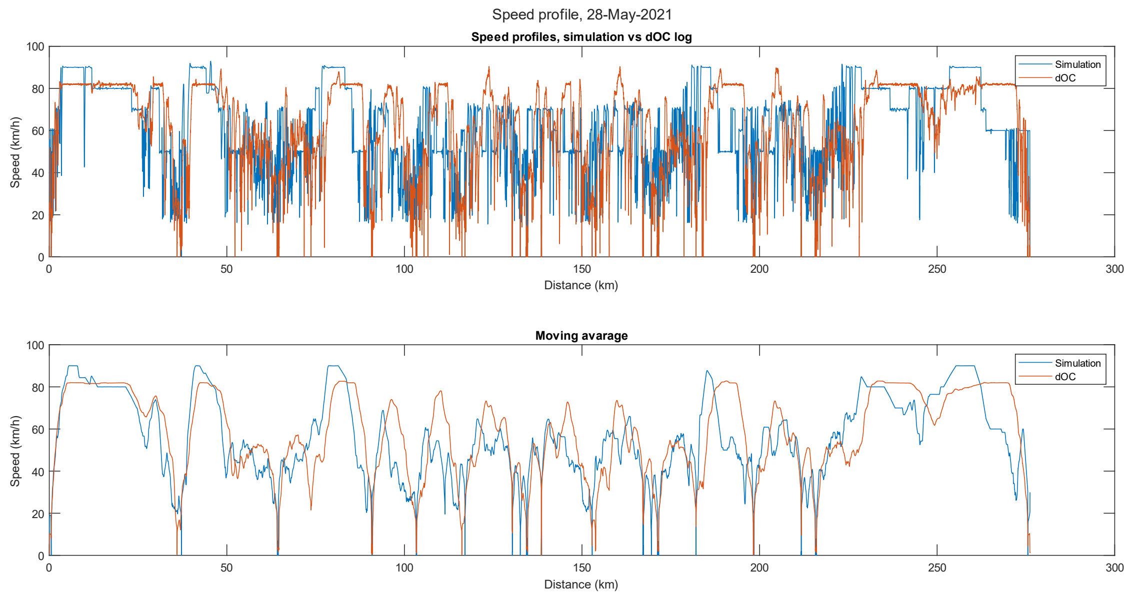

Figure 4-8. Speed log for Mission 2021-May-28. The upper subplot presents the measured signal. A moving average filter applied on the measured signal results in the signal presented in the lower subplot.

4.3.2 Stochastic model evaluation

To evaluate the stochastic models developed under Section 3.3, mission stops and mass logs are generated. For each dOC, the fields Payload and mission stop are now overwritten by the generated mass and mission stops. The values of those fields are generated from the stochastic model's *Payload and Mission stop.* The models and parameter values used to generate the samples are those presented in Section 3.3. To ease the reading, the notation *generated dOC* refers to dOCs with modified payload and mission stop fields. Energy consumption in simulations using the generated dOCs are to be compared against log data and the simulated dOCs. The results are shown in Figure 4-9.

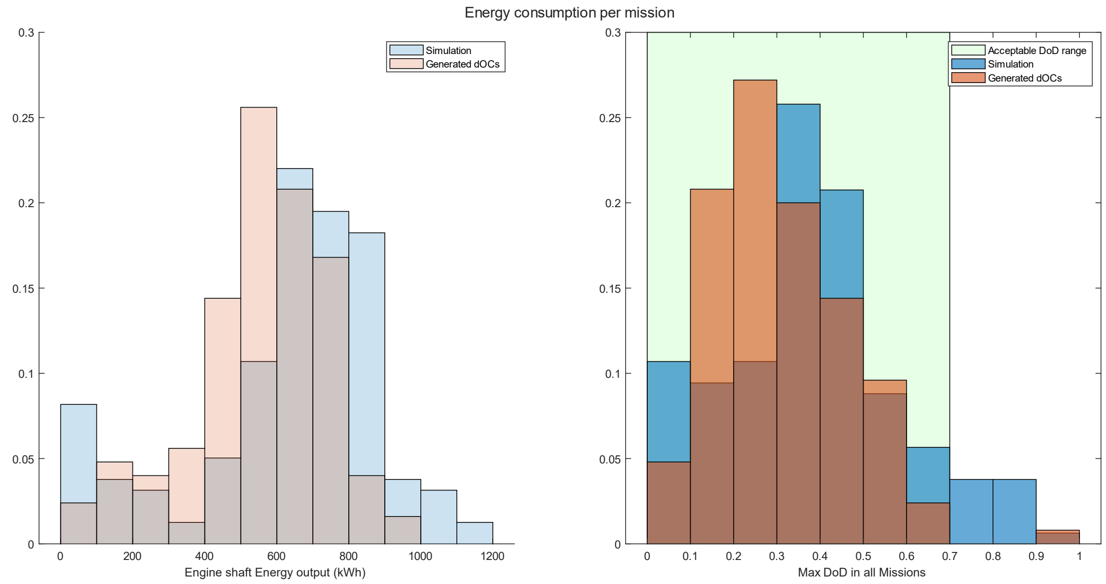

Figure 4-9. The left subplot displays the engine shaft energy output. It shows that the generated dOCs are on average running a bit too easily. The right subplot displays the DoD. It shows that the DoD of generated dOCs is on average a bit low.

Looking at the histograms, it seems like the generated dOCs do in general have a lower energy consumption. The shape is relatively similar but shifted with about 100 kWh. To find the cause, a comparison of the generated mass and the logged mass is conducted. Recalling from Section 3.3.1, four processes should be considered, distance travelled in state, transition in between states, payload magnitude in each state and initial state. First, the distance travelled in state was assumed to be equal for all states. The distance driven within states over all the missions is presented in Figure 4-10.

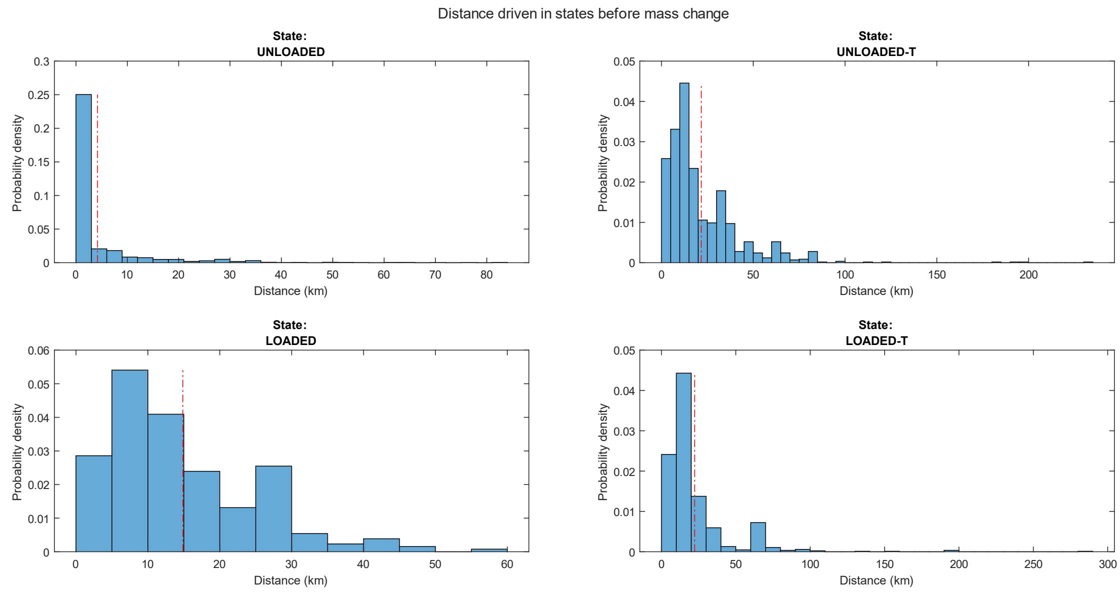

Figure 4-10. Four subplots present the distribution of distance travelled within state for each state.

The difference in distance driven within state are noticeable. The driver does stay in state LOADED-T about 5 times longer than within the state UNLOADED. These states do differ in GCW by about a factor of 4 (about 15 and 60 tonnes respectively depending on the kerb weight of the vehicle). Now, the mass resulting from the sOC model is compared to the dOC-filtered mass in Figure 4-11. From this figure, it is possible to evaluate one out of the three remaining processes, the payload magnitude. The payload magnitude stochastic model is representative if the shape of each state is similar comparing the dOCs and the generated dOCs. Since the two unloaded states take the constant values of 0 and 6.22 tonnes (for an explanation, see Section 3.3.1) only the loaded states' distributions are presented.

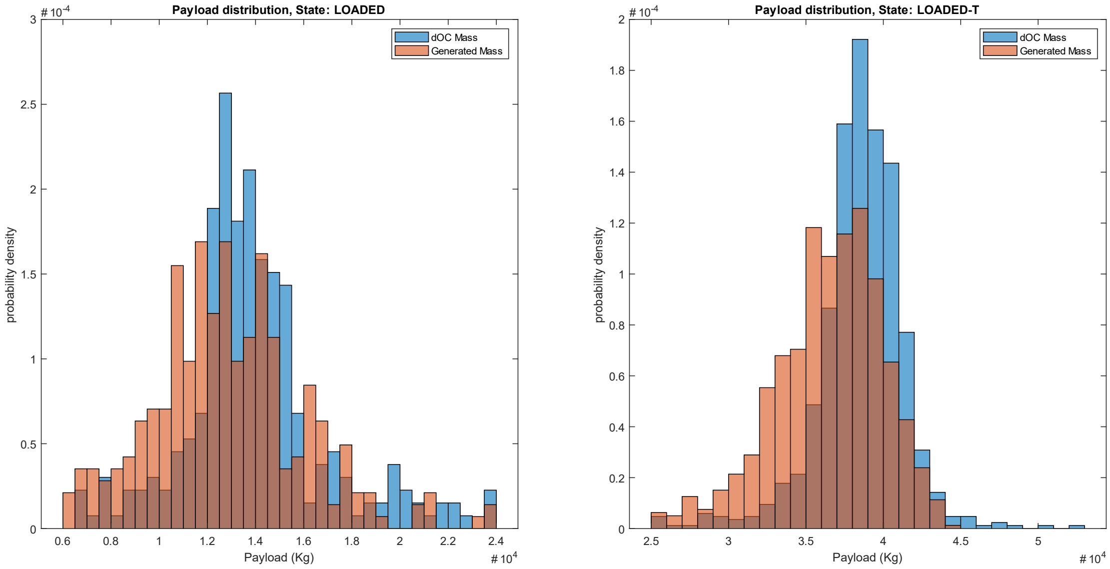

Figure 4-11. Comparison of dOC and generated dOC mass logs for the two loaded states.

The shape is relatively similar indicating that the payload magnitude is well represented by our models. The two other processes, transition in between states and initial state modelling are correctly modelled if the weight of each state is similar comparing the dOCs and the generated dOCs. The weight of each state is presented in Figure 4-12.

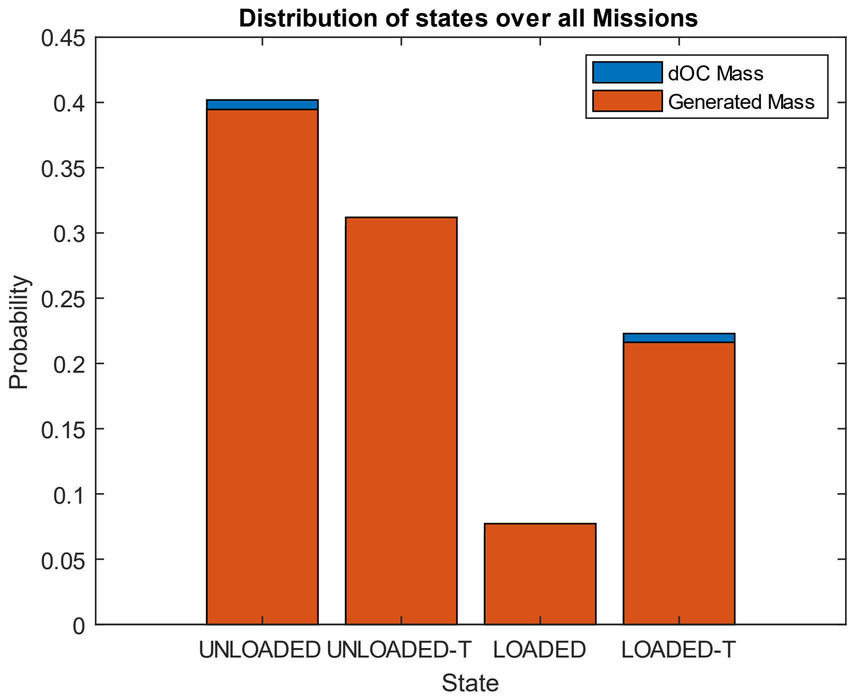

Figure 4-12. Comparison of dOC and generated dOC weights. The weights correspond to the number of times transitioning to state and starting in the state.

The weights are very similar, indicating that our model have fit the data well. Now that all the four processes have been examined it is fair to say the shift in Figure 4-9 is likely a result of the incorrect assumption made regarding equal distance driven within state.

5 Conclusions and Future work

5.1 Conclusions

Explain main conclusions & results. Be careful to include description of how you have met each of the objectives and deliverables. Short and often suitable on bullet form. (If more than 0.5..1 page, consider to move to other chapter, such as Result or Discussion.)

- By including data analytics in the OC format, some new system dynamics have been discovered. A mass trace is now included and a model for mission stops. Also, one can see the importance mass plays in energy consumption. Just from one incorrect assumption, one can see a noticeable shift in energy consumption.
- A large portion of the work has been to build a framework that transforms log data into dOCs. This framework will prove very useful for future studies within the field as it not only saves time but also includes the dynamics of a transport mission that has not been included before.
- From Section 4.2, one now has an idea of how well a BEV can perform. The number of missions classified as failed in terms of DoD is not neglectable. We can from this result argue that a BEV cannot replace the FH16 without alteration of the transport mission. Vehicles of other transport missions could use the same framework developed to investigate if those can be replaced by a BEV.

5.2 Future work

To expand the use of our models, extensive validation of the models should be conducted. Given that the validation proves successful, the models do have other potential use cases. For example, they can assist in range prediction for vehicles in operation and also give valuable insights into vehicle usage. It is reasonable to believe that the models developed are not a perfect representation of all transport missions. Just from this study, numerous assumptions have been proven invalid after evaluation. For example, the payload sOC model. As discussed in Section 4.2.1, a new model of the distance travelled in state should preferably be developed. Also, the inaccuracy of the model fit for the mission stop sOC model should be further investigated, see Section 3.3.2. A couple of models even require implementation. A model for EV-Recharging and a driver decision-making algorithm is presented in the present thesis and the author recommends coming authors to implement and validate these models further. They have the possibility to produce a more precise measure of DoD, enabling analysis of probable mission success rate concerning DoD.

From the literature studies, improvements of one model were recognized, the traffic light sOC model. The author was in contact with Göteborgs Trafikkontor regarding statistics of traffic lights without any success. But given that data is available, the modal proposal is the following:
Traffic signs stand still time should preferably be modelled by equation (5-1).

$$\tilde{T}_k = T_k x \qquad (5\text{-}1)$$

Here, T_k is the uniformly distributed variable described in equation (2-3), x is a Bernoulli distributed random variable with probability p, and $\tilde{T}_k$ is the new random variable representing standstill time at traffic lights. The current model does not model the occurrence of green lights, it assumes all traffic lights to be red. But the new and purposed model does however model both green and red lights. It is important to note that the dynamics of traffic lights could be even further developed. Some traffic lights are movement-sensitive and phenomena such as the green wave are impacting the probability of encountering red and green lights.

In Section 4.3.1, the mission total time was examined. The result showed that simulations do vary quite a bit from the logged vehicle. Probable causes for this are listed below:

- Load on/off event is estimated to take 300 seconds, which might be an inaccurate estimate for certain missions.
- VehProps Mission state machine gets stuck due to zero crossings.
- Vehicle limitations such as max power and max torque might reduce the speed of the vehicle for certain missions.
- The Vehprop driver model might not perfectly represent the driver of the logged vehicle.
- Idling without any action is not captured in the dOC format. For example, the driver might be idling at the mine site while talking to colleagues. That is not accounted for in the dOC format.
- The standstill time at red lights and stop signs is estimated. A lucky driver might never stop at a red light.
- VehProp does not model traffic even though the dOC format provides such data. Trivially, the logged vehicle is affected by the traffic density which might vary from day to day.

Also, the OC format is still in development. New models are continuously being developed that will make simulations match the logged vehicles even more accurately. In Section 4.3.1, the linear offset for energy consumption comparing simulation results to the logged vehicle was examined. The result showed that simulations could be offset by up to 0.3 kWh/km which implies that a mission operated under 300 km could have a linear offset of 90 kWh. After consultation with Klimator, a market-leading digital road weather solution provider, a day of extraordinarily poor road conditions was now known, that is the 17th of February 2021. A comparison between that day and a day during summer, the 10th of August 2021, to display the impact of road conditions on energy consumption is presented in Figure 5-1.

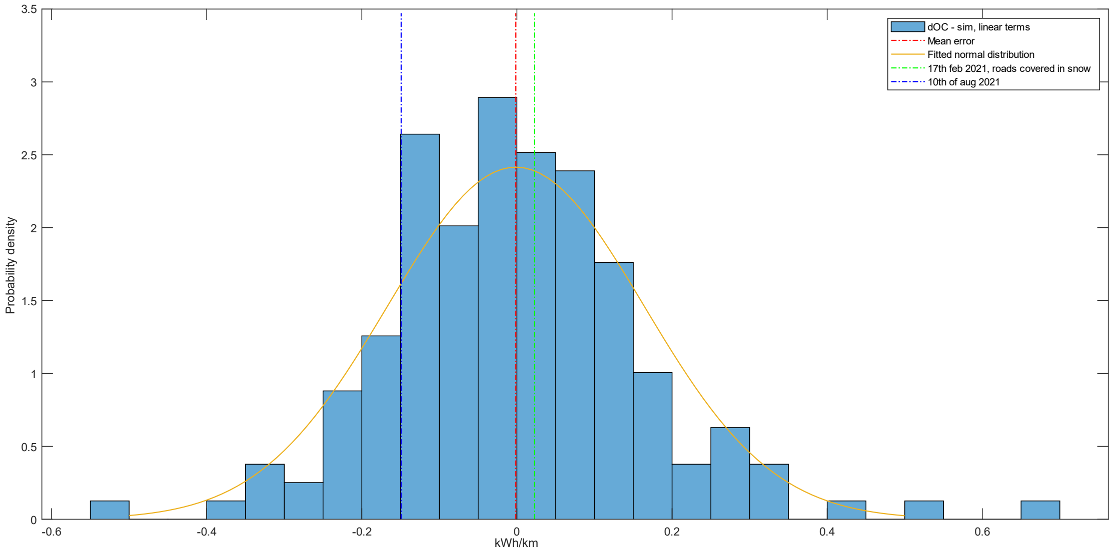

Figure 5-1. Linear term comparison between a mission performed under snowy road conditions and a mission performed during the summer.

As anticipated, the summer day has its energy consumption overestimated in simulation whereas, during the 10th of February, the opposite is true. But two missions are not sufficient to draw any conclusions, therefore the author recommends coming authors to investigate this further. Studies have shown that road weather conditions can have huge impacts on energy efficiency for road vehicles [25] and are likely one of the causes of the linear offset that certain missions experience in simulation.

APPENDIX A

A.1 Multimodal Normal distributions.

First, collect one year's worth of mass logs and plot the occurrence in a histogram. Second, fitting 4 Normal distributions, one to each load case, results in the following characteristics, see Table A-1 where ω is the weight of each distribution

Table A-1. Characteristic parameters from fitting four normal distributions to GCW data, one for each state.

	μ	σ	ω
UNLOADED	15758.9	1266.99	0.1935
UNLOADED-T	22437.5	1129.02	0.4099
LOADED	29028.6	1672.52	0.1077
LOADED-T	53970.3	2045.13	0.2206

The resulting multimodal distribution can be seen in Figure A-1

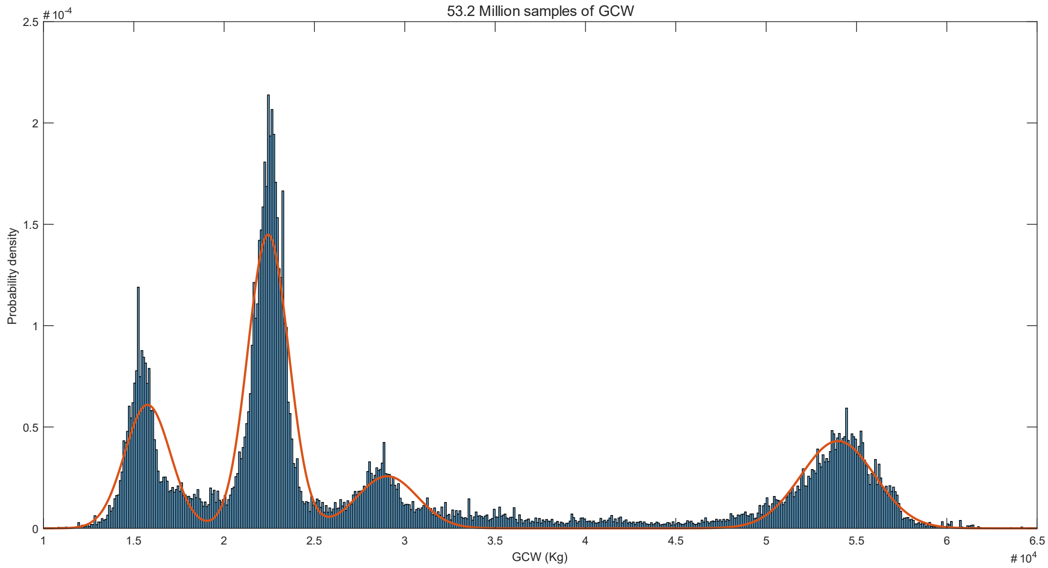

Figure A-1. The histogram displays the distribution of all GCW data available. A multimodal distribution consisting of 4 normal distributions is fitted to the GCW data.

The probability density function of the multimodal distribution is presented in equation (A-1)

$$f(x) = \sum_{i=1}^{4} \omega_i f_{n(x,\mu_i,\sigma_i)} \qquad \text{A-1}$$

Here, subscript i is an integer value representing the four different states. The probability density function $f_{n(x,\mu_i,\sigma_i)}$ is presented in equation (A-2).

$$f_{n(x,\mu_i,\sigma_i)} = \frac{1}{\sigma_i\sqrt{2\pi}}\, e^{-\frac{1}{2}\left(\frac{x-\mu_i}{\sigma_i}\right)^2} \qquad \text{A-2}$$

No further analysis of this result is provided.

A. 2 Queueing theory

Queueing theory is the mathematical study of waiting lines. The main purpose of queueing theory is to quantify and predict queue time and queue length using a set of parameters. This thesis makes use of queues with Kendall's notation $(M/M/S)$: $(FCFS/\infty/\infty)$ to describe queues at recharging stations. The entries of the Kendall notation are briefly described in the list below:

- $\boldsymbol{M}$: Inter-arrival time. Arriving vehicles are modelled as a Poisson process.
- $\boldsymbol{M}$: Exponential service time. Vehicle service time is modelled as a Poisson process.
- $\boldsymbol{S}$: Number of service channels. A charging station with five connectors has five service channels.
- $\boldsymbol{FCFS}$: First Come First Served. Vehicles are served in the order of arrival.
- ∞: The calling population. That is the number of BEVs that could charge at a specific station. It is assumed to be infinite.
- ∞: The maximum number of vehicles in the waiting line before customers choose another station. It is assumed to be infinite.

A. 3 Threshold filter

A binary threshold filter marks data as either above or below the threshold, 1 or 0. Given a threshold T, the binary random variable is defined by the value of the random variable x(t), see equation (A-3).

$$X(t) = \begin{cases} 1, & if x(t) > T \\ 0, & if x(t) < T \end{cases} \qquad \text{A-3}$$

A. 4 Spike filter

A spike filter counts the number of consecutive samples encountered with the same Binary value. If the number of consecutive samples is less than T_s, the opposite value is assigned to the whole sequence. Each sequence of consecutive identical samples is denoted B_i and the number of elements in B_i is denoted n_i. The filter equation is presented in equation (A-4).

$$B_i = \begin{cases} B_i, & if\ n_i > T_s \\ B_i^C, & if\ n_i < T_s \end{cases}, \qquad for\ i = 1,2,..,k \qquad \text{A-4}$$

The resulting filtered signal is the composition of every sequence $X_f(t) = \{B_1, \dots, B_k\}$.

A. 5 Marked Poisson Process

The marked Poisson process models randomly scattered discrete events in the mathematical space, where each event is independent of the other. For this thesis, the space is reduced to the positive real axis, distance. With the rate of occurrence λ one can calculate the number of events expected up until the distance t using equation (A-5).

$$P(N(t) = k) = P_\lambda(t) = \frac{(\lambda t)^k}{k!} e^{-\lambda t}, \qquad k \geq 0 \qquad \text{A-5}$$

To illustrate, five Poisson distributions are presented in Figure A-2 using $t = 1$.

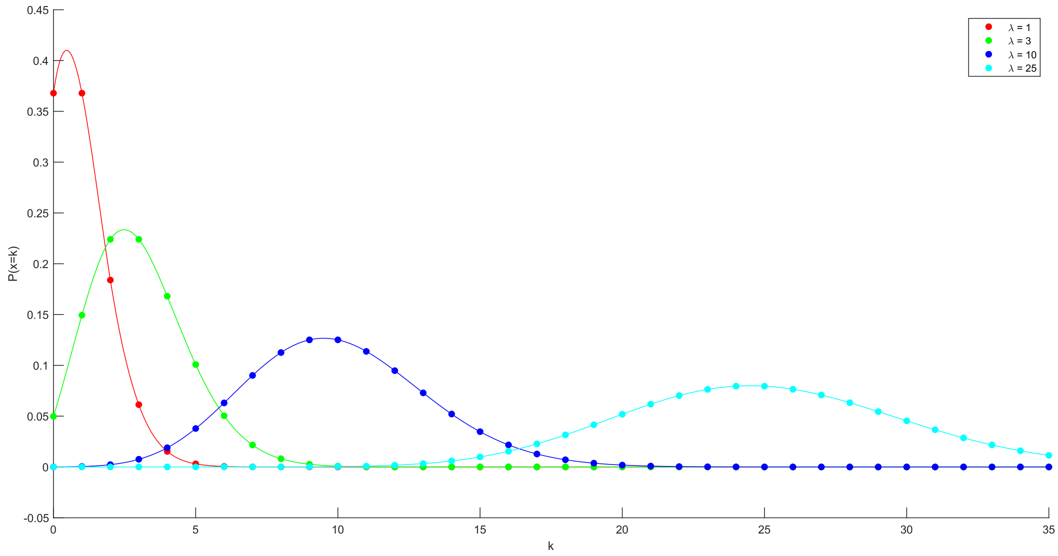

Figure A-2. Poisson distribution with five different λ for $t = 1$.

The probability of an event occurring if driving the distance t is presented in equation (A-6).

$$P(T \leq t) = 1 - P(N(t) = 0) = 1 - \mathrm{e}^{-\lambda t} \tag{A-6}$$

This process is repeatably used throughout this thesis and is usually the initiator of a certain event. Meaning that the marked Poisson process models the occurrence of events, not the effect of events.

A. 6 Gamma distribution

A gamma distribution is parameterized by the shape and rate parameters $\alpha, \beta > 0$ with the probability density function $\Gamma(\alpha, \beta)$, see equation (A-7).

$$f(x;\ \alpha, \beta) = \frac{\beta^{\alpha}}{\Gamma(\alpha)} x^{\alpha-1} e^{-\beta x}, \qquad x > 0 \tag{A-7}$$

The gamma function $\Gamma(\cdot)$ is defined by equation (A-8)

$$\Gamma(z) = \int_0^{\infty} \mathrm{x}^{\mathrm{z}-1}\, \mathrm{e}^{-\mathrm{x}} \mathrm{dx}, \qquad Re(z) > 0 \tag{A-8}$$

To illustrate, by fixating one parameter at a time, one can see the impact of each parameter in the distributions presented in Figure A-3.

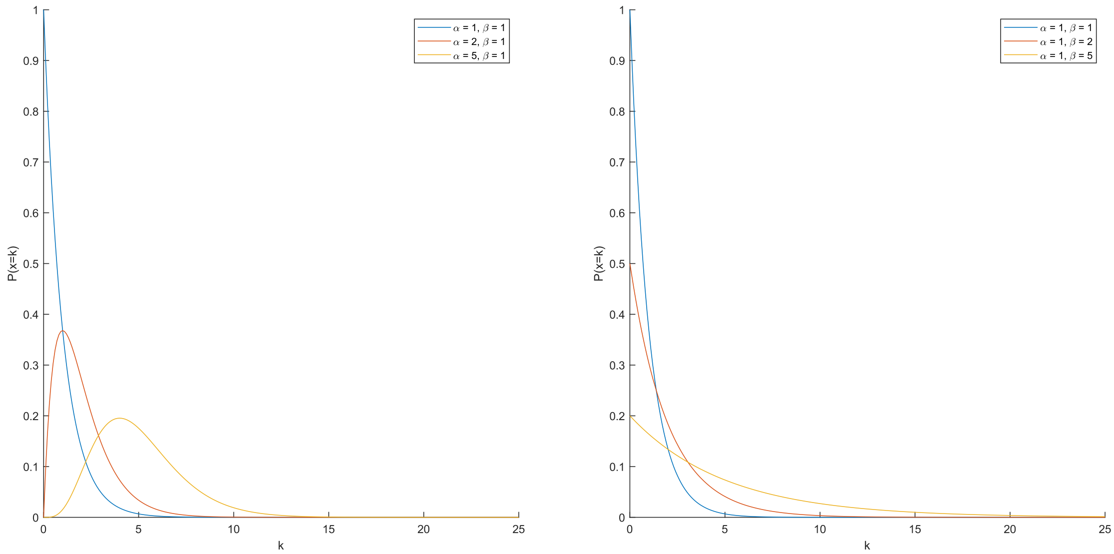

Figure A-3. Gamma distributions with different parameters display the impact of each parameter.

6 References

[1] Sheth, N. Sethia, K. Srinivas, S. (2011): *Mindful consumption: a customer-centric approach to sustainability*. Atlanta, USA: Emory University.

[2] European commision. (Accessed jan. 09, 2023): *Vehicle Energy Consumption calculation Tool – Vecto*. ec.europa. https://climate.ec.europa.eu/eu-action/transport-emissions/road-transport-reducing-co2-emissions-vehicles/vehicle-energy-consumption-calculation-tool-vecto_en#documentation.

[3] Åkerinäringen. (2019): *Färdplan för fossilfri konkurrenskraft.*

[4] Paoli, L. Gül, T. (2022): *Electric cars fend off supply chenges to more than double global sales.* IEA.

[5] European Union. (2019): *REGULATION (EU) 2019/1242 OF THE EUROPEAN PARLIAMENT AND OF THE COUNCIL of 20 June 2019 setting CO2 emission performance standards for new heavy-duty vehicles and amending Regulations (EC) No 595/2009 and (EU) 2018/956 of the European Parliament and of the Council and Council Directive 96/53/EC.*

[6] Buis, A. (2022): *Steamy Relationships: How Atmospheric Water Vapor Amplifies Earth's Greenhouse Effect.* NASA's Jet Propulsion Laboratory.

[7] Our World in Data. (Accessed Jan. 09, 2023): *Annual* co_2 *emissions*. ourworldindata. https://ourworldindata.org/grapher/annual-co2-emissions-per-country?facet=none&country=~OWID_WRL.

[8] United Nations. (2019): *Climate Justice.*

[9] Nordström, E. (2020): *Advanced Modelling and Energy Efficiency Prediction for Road Vehicles*. Umeå, Sweden: Umeå University.

[10] Romano, L. (2021): *Mathematical modelling of operating cycles for road vehicles*. Göteborg, Sweden: Chalmers University of Technology.

[11] Pettersson, P. (2019): *Operating cycle representations for road vehicles.* Göteborg, Sweden: Chalmers University of Technology.

[12] Sahoo, P. Soltani, S. Wong, A. (1988): A Survey of Thresholding Techniques.

[13] Stanley, G. (Accessed jan. 09, 2023): *Spike Filtering.* gregstanleyandassociates. https://gregstanleyandassociates.com/whitepapers/FaultDiagnosis/Filtering/Spike-Filter/spike-filter.html.

[14] U.S. Geological Survey. (2022): *Mineral commodity summaries 2022.* Reston, Virginia, USA.

[15] Here developer. (Accessed Jan. 09, 2023): *Country support*. Developer.here *https://developer.here.com/documentation/places/dev_guide/topics/coverage-information.html.*

[16] European Comission. (Accessed jan. 09, 2023): *Recharging systems. Ec.europa. https://alternative-fuels-observatory.ec.europa.eu/general-information/recharging-systems.*

[17] TomTom. (Accessed jan. 09, 2023): *Gothenburg traffic. tomtom. https://www.tomtom.com/traffic-index/gothenburg-traffic.*

[18] Weber, P. Braaksma, J. (2000): *Towards a North American Geometric Design Standard for Speed Humps.*

[19] Johannesson, P. Podgórski, K. Rychlik, I. (2016): *Modelling roughness of road profiles on parallel tracks using roughness indicators.*

[20] Vackert Väder. (Accessed jan. 09, 2023): *Väder Göteborg.* Vackertvader. https://www.vackertvader.se/g%C3%B6teborg/klimat-och-temperatur.

[21] Pettersson, P. Berglund, S. Jacobson, B. et al (2018). *A proposal for an operating cycle description format for road transport missions*.

[22] Virta. (Accessed jan. 09, 2023): Virta. www.virta.global.

[23] Balaraaman, P. Chandrasekaran, P. (2021): *Influence of loading cycle time on the performance of hydraulic excavator in a construction site.* Chennai, India: SRM Institute of Science and Technology.

[24] Pettersson, P. Johannesson, P., Jacobson, B. Bruzelius, F. Fast, L., Berglund, S. (2019): *A statistical operating cycle description for prediction of road vehicles' energy consumption.*

[25] Nordin, L. (2015): *Energy Efficiency in Winter Road Maintenance.* Department of Earth Sciences, University of Gothenburg, Sweden.